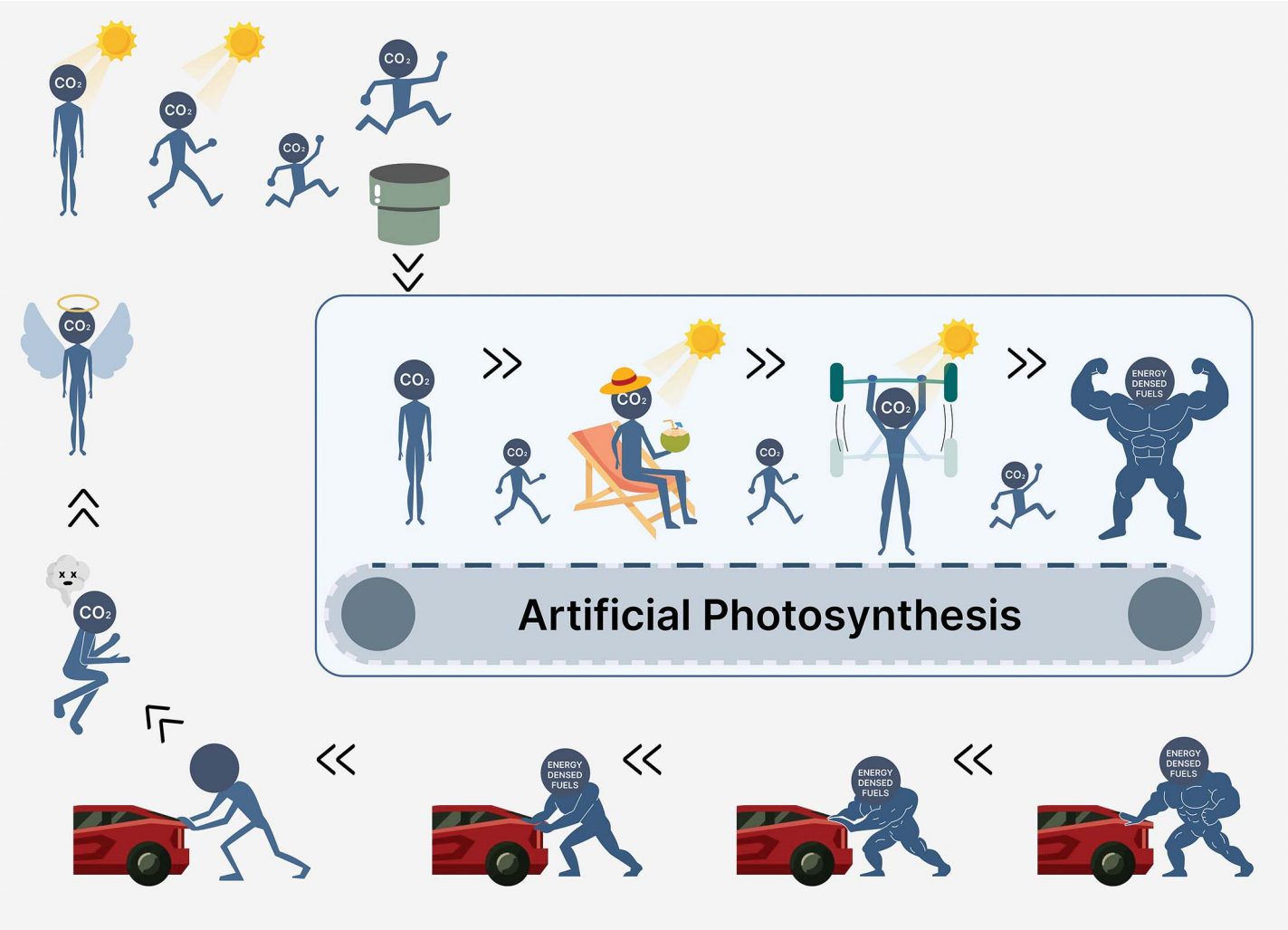

Showcasing research from Professor Wang's laboratory, Graduate School of Engineering, Nagoya University, Nagoya, Japan & Pornrungroj's laboratory, Faculty of Engineering, Chulalongkorn University, Bangkok, Thailand.

Artificial photosynthetic processes using carbon dioxide, water and sunlight: can they power a sustainable future?

This Perspective explores the promise and challenges of artificial photosynthesis, where sunlight, water, and carbon dioxide are converted into energy-rich fuels and chemicals. We assess the current status of solar-driven CO_2 conversion technologies, highlighting the techno-economic barriers of capture, separation and scale-up. By connecting laboratory progress with practical considerations, we propose opportunities that could bring these systems closer to real-world application. Our analysis aims to provide a clearer picture of the pathways toward sustainable solar fuel production in the future.

Image reproduced by permission of Qian Wang and Chanon Pornrungroj from *Chem. Sci.*, 2025, **16**, 18990.

As featured in:

See Qian Wang and Chanon Pornrungroj, *Chem. Sci.*, 2025, **16**, 18990.

ROYAL SOCIETY OF CHEMISTRY

15 YEARS ANNIVERSARY

rsc.li/chemical-science

Registered charity number: 207890

Chemical Science

ROYAL SOCIETY OF CHEMISTRY

PERSPECTIVE

View Article Online
View Journal | View Issue

Cite this: *Chem. Sci.*, 2025, **16**, 18990

All publication charges for this article have been paid for by the Royal Society of Chemistry

Artificial photosynthetic processes using carbon dioxide, water and sunlight: can they power a sustainable future?

Qian Wang *[a] and Chanon Pornrungroj *[bcd]

Solar-driven carbon dioxide reduction (CO_2RR) mimics natural photosynthesis by harnessing sunlight to convert water and CO_2 into chemicals, thereby enabling the storage of solar energy in energy-dense molecules for on-demand use. With the accelerated advancement of solar-driven CO_2-to-chemicals conversion technologies, this approach holds promise for contributing to the realisation of a zero-carbon society, a target increasingly prioritised by governments worldwide. Here, we argue that despite these promising developments, substantial challenges persist at both the material and system levels, extending beyond the catalytic process itself to include upstream CO_2 capture and downstream product separation and purification. We also present a techno-economic assessment of current solar-driven CO_2RR platforms and conclude that they remain well below the thresholds necessary for commercial-scale deployment. To address this gap, we propose several directions for future progress. From a fundamental perspective, the integration of machine learning models and data-driven approaches, in conjunction with *operando* spectroscopic techniques, may accelerate the discovery and optimisation of materials by providing rational design principles. From a practical standpoint, the deployment of CO_2RR systems in non-traditional environments, such as desert regions or aquatic platforms, and their coupling with alternative oxidation reactions (*e.g.*, waste photoreforming) may improve system viability by reducing the capital cost and extracting added value from oxidation products. We hope that these analyses and proposals will help advance next-generation solar fuel production systems and enhance their prospects for real-world applications.

Received 31st May 2025
Accepted 22nd September 2025

DOI: 10.1039/d5sc03976b

rsc.li/chemical-science

[a]*Graduate School of Engineering, Nagoya University, Furo-cho, Chikusa-ku, Nagoya 464-8603, Japan. E-mail: wang.qian@material.nagoya-u.ac.jp*

[b]*Department of Chemical Engineering, Faculty of Engineering, Chulalongkorn University, Bangkok 10330, Thailand. E-mail: chanon.po@chula.ac.th*

[c]*Photocatalysts for Clean Environment and Energy Research Unit, Faculty of Science, Chulalongkorn University, 254 Phayathai Road, Pathumwan, Bangkok 10330, Thailand*

[d]*Bio-Circular-Green-economy Technology & Engineering Center (BCGeTEC), Faculty of Engineering, Chulalongkorn University, Bangkok 10330, Thailand*

Qian Wang

Qian Wang is currently a Professor at Nagoya University, Japan. She received her PhD in 2014 from the University of Tokyo and continued her postdoctoral research at the same institution. In 2018, she was awarded a Marie Skłodowska-Curie Fellowship, under which she initiated her research at the University of Cambridge. She joined Nagoya University as an Associate Professor in 2021 and was promoted to Professor in 2025, where she established her research group. Her team focuses on the development of novel materials, strategies and technologies for the conversion of solar energy into renewable fuels through artificial photosynthesis.

Chanon Pornrungroj

Chanon Pornrungroj received his BS (2015) and MS (2017) in Chemistry from Tohoku University, Japan, and his PhD (2023) in Chemistry from the University of Cambridge, UK. He started his independent career in 2023 as a lecturer at Chulalongkorn University, Thailand. His research interests include solar energy conversion, (photo) electrocatalysis, and hybrid solar-driven processes, with a focus on integrating catalytic performance and system design to address the water–energy–food–environment nexus.

1. Introduction

In response to the rising levels of anthropogenic CO_2 emissions, which are outpacing the capacity of the natural carbon cycle and contributing to adverse global environmental changes,[1] scientists and engineers have focused intense research, development and deployment efforts over the past decade on the solar-driven conversion of CO_2 into fuels and value-added chemicals. This approach, inspired by the design of natural photosynthesis, involves the use of sunlight-irradiated semiconductors to generate holes that oxidise water into oxygen, releasing protons (Fig. 1). Simultaneously, electrons reduce these protons and CO_2 into chemical products such as hydrogen (H_2), carbon monoxide (CO), formic acid (HCOOH), methane (CH_4) and other carbon-based fuels. The overall reaction sequence of "artificial photosynthesis" stores solar energy by breaking and forming chemical bonds in water and CO_2, resulting in the evolution of oxygen and the formation of energy-rich carbon-based products. It offers a promising strategy for simultaneously addressing several critical challenges: (1) capturing and storing intermittent and unevenly distributed solar energy in chemical form, which is easier to store, transport and utilise; (2) allowing the creation of closed carbon cycles in which CO_2 emissions are captured and converted back into fuels, thereby contributing to emission reduction and net-zero goal; and (3) offering sustainable alternatives to fossil fuels, supporting long-term energy security and reducing reliance on non-renewable resources.

One established approach to solar-driven CO_2 conversion involves a two-step process that combines photovoltaic electricity generation with an electrolytic CO_2RR system (PV-EC) (Fig. 1). In this configuration, solar energy is initially converted into electricity through photovoltaic devices, which subsequently power the electrolysis system. A benchmark example is given by a copper/tin-oxide catalyst powered by a III–V $InGaP_2$/InGaAs/Ge triple-junction solar cell, which achieved a solar-to-fuel conversion efficiency (STF) of 19.9% with a faradaic efficiency of 98.9% for CO_2-to-CO conversion under simulated one sun irradiation (standard air mass 1.5 global, AM 1.5G, 100 mW cm^{-2}).[2]

While this method is technically feasible using current technologies, a potentially more cost-effective and integrated alternative is the development of single-device systems that use semiconductors as both light absorbers and energy converters.[3–5] Such a system can be realised *via* photoelectrochemical (PEC) or photocatalytic (PC) processes, enabling the direct conversion of sunlight into chemical energy (Fig. 1).[5] For instance, several UV-driven particulate photocatalysts, such as metal-ion-doped $NaTaO_3$ and $SrTiO_3$,[6,7] have demonstrated selective CO_2RR to CO upon loading Ag as a catalyst, while simultaneously oxidising water to O_2. These systems are considerably simpler than PV-EC configurations because the reactions occur directly at the semiconductor/liquid interface,[8] eliminating the need for external wiring and reducing system complexity and cost. Nonetheless, the STFs obtained using these UV-responsive photocatalysts are limited due to their narrow absorption range,[9] as UV light comprises less than 5% of the solar spectrum. In semiconductor-powder-based artificial photosynthesis, photons with energies greater than the bandgap excite electrons from the valence band to the conduction band, leaving holes in the valence band (Fig. 2a). The excited electrons drive the CO_2RR, while the holes initiate the water oxidation reaction to evolve O_2. For this process to occur, the conduction-band minimum must be positioned more negatively than the standard CO_2RR potential, and the valence-band maximum must be positioned more positively than the water oxidation potential. Satisfying these thermodynamic requirements while simultaneously enabling broad-

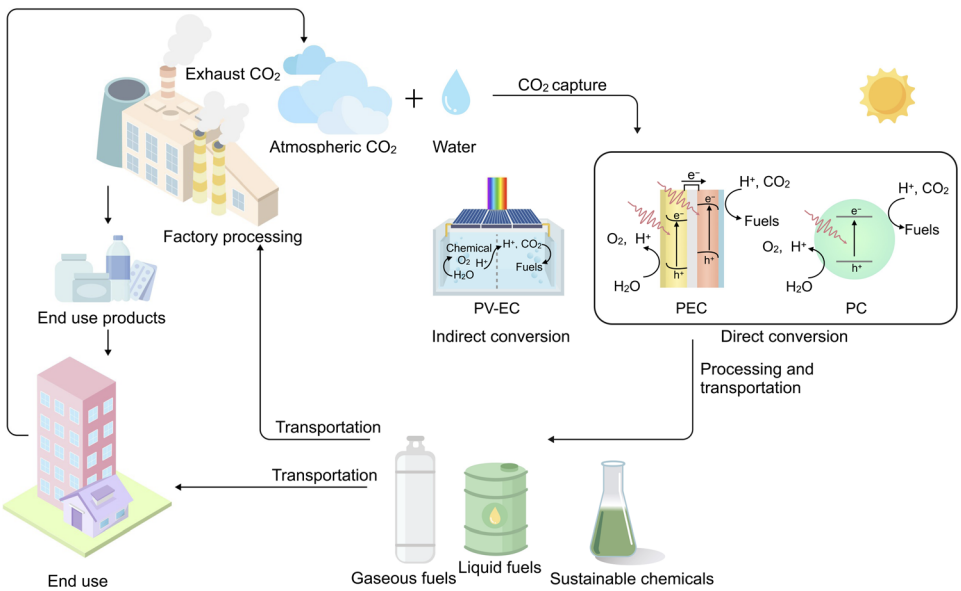

Fig. 1 Solar-powered CO_2RR technology and the sustainable carbon energy cycle.

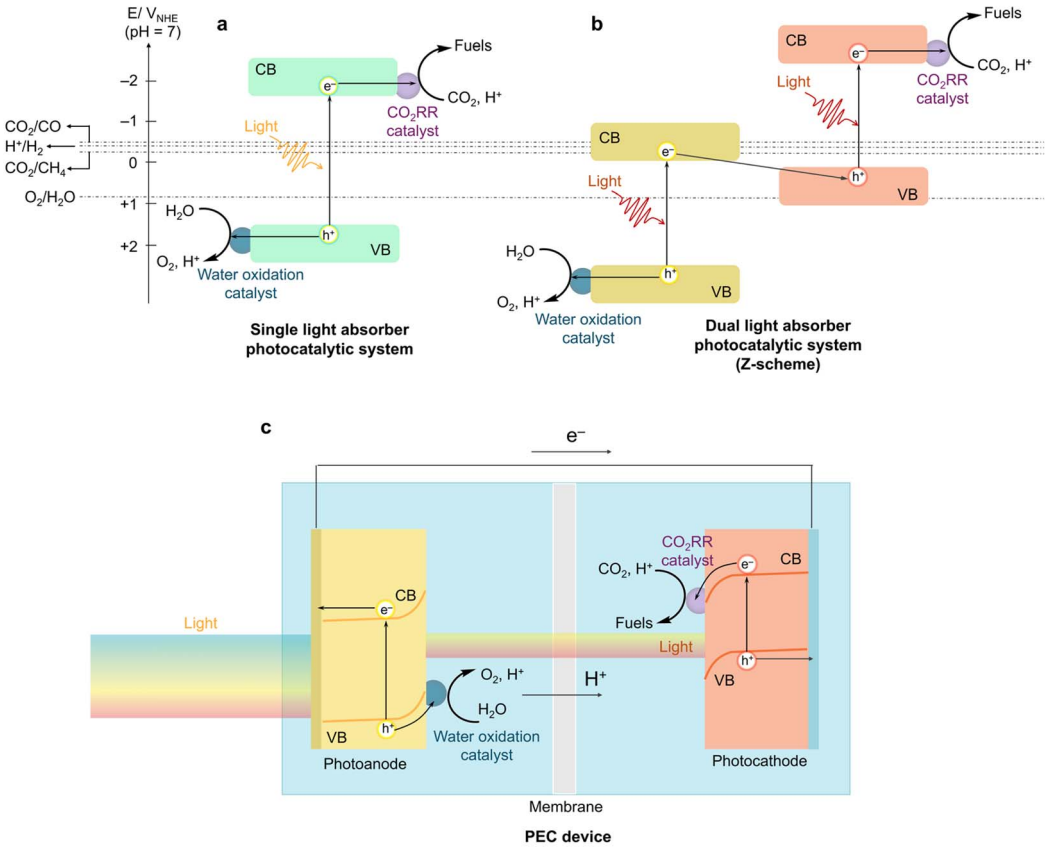

Fig. 2 Schematic of (a) a single light absorber photocatalytic system, (b) a dual light absorber photocatalytic system (*Z*-scheme) and (c) a tandem PEC cell under illumination. CB: conduction band; VB: valence band.

spectrum light absorption within a single semiconductor remains a major challenge.

An alternative approach involves spatially separating the reduction and oxidation reactions onto two distinct semiconductors, constructing a *Z*-scheme system analogous to photosystem I and photosystem II in natural photosynthesis (Fig. 2b). This configuration offers a key advantage by distributing the overall voltage requirement across two light absorbers, thereby lowering the kinetic demands on each semiconductor and enabling the use of narrow-bandgap materials that are active for either CO_2RR or water oxidation.[10] For example, a *Z*-scheme system integrating lanthanum- and rhodium-doped $SrTiO_3$ ($SrTiO_3$:La,Rh), modified with phosphonated Co(II) bis(terpyridine) for CO_2RR, and molybdenum-doped $BiVO_4$ ($BiVO_4$:Mo) for water oxidation, bridged by a gold layer, achieved an STF of 0.08 ± 0.01% for formate production with a selectivity of 97 ± 3%.[11] Nonetheless, recombination of photogenerated holes in the CO_2RR photocatalyst and electrons in the water-oxidation photocatalyst, both of which are not utilised in the redox reactions, limits the maximum theoretical quantum efficiency of such systems compared to single-light-absorber configurations. In addition, because reduction and oxidation occur within the same reaction cell, undesirable back-reactions, such as the recombination of products or their reaction with photogenerated charge carriers under illumination, must be minimized.

Likewise, tandem PEC architectures, which employ two distinct light absorbers (a photocathode and a photoanode) connected *via* external wiring with an ohmic contact (Fig. 2c), represent a promising approach for achieving high-efficiency solar fuel conversion. To perform the redox reactions while avoiding charge-carrier recombination, photogenerated electrons and holes in the semiconductors must be transported to the semiconductor/electrolyte interface, where they react with solution-phase species present at the surface. The photogenerated electrons in photocathode migrate to the photocathode/electrolyte interface to reduce CO_2, while photogenerated holes in photoanode drift to the photoanode/electrolyte interface to oxidise water and release O_2. The holes in the photocathode and electrons in the photoanode recombine at the ohmic contact. At these interfaces, electron transfer is accompanied by energy losses arising from both concentration gradients and kinetic overpotentials required to drive the half-reactions.[8]

By selecting light absorbers with complementary spectral responses, tandem PEC devices can utilise a broader fraction of the solar spectrum while generating sufficient photovoltage to couple CO_2RR with water oxidation. In contrast to common *Z*-

scheme photocatalytic systems, where two particulate photocatalysts are simply mixed and compete for the same portion of incident sunlight, PEC systems can be configured in a tandem arrangement by stacking two photoelectrodes so that the photoanode (or photocathode) with the larger band gap is placed in front, and the photocathode (or photoanode) with the smaller band gap is positioned behind (Fig. 2c). This configuration minimises spectral competition and enables more efficient utilisation of the solar spectrum.[8,12] A further operational advantage of the PEC approach lies in the capacity to spatially separate the oxidation and reduction half-reactions into distinct compartments, which significantly suppresses back-reactions.

The successful realisation of such integrated PEC systems demands careful optimisation of the interplay between the light-harvesting component, the ion-selective membrane and the overall device configuration.[12] The light absorber must maximise photocurrent density and provide sufficient photovoltage for the target redox reactions; the membrane must limit produced gas crossover and minimise ohmic losses; and the cell architecture must ensure efficient ion transport in the electrolyte phase. The overall reaction efficiency is determined by both the photovoltage and the photocurrent density of the light absorber, with the maximum attainable photocurrent density typically decreasing as the number of junctions increases.[12] Examples of bias-free PEC systems that incorporate dual semiconductors, each forming a semiconductor/liquid junction, remain rare. One notable example achieved the co-production of formate and O_2 from CO_2 and water by coupling an InP/Ru-complex hybrid photocathode with a reduced $SrTiO_3$ photoanode, yielding an STF of 0.08%.[13]

Despite significant investment in solar-driven CO_2RR research and the development of numerous semiconductor materials, (electro)catalysts and cell configurations, no prototype system has yet met the combined criteria of efficiency, selectivity, scalability, long-term stability and cost-effectiveness required for practical deployment. Significant challenges related to energy conversion efficiency and reaction selectivity must be addressed for solar-driven CO_2RR to become a practical and viable approach for solar fuel production and to make a real impact at scale.

The primary objective is the solar-driven conversion of CO_2, either emitted from industrial sources or captured from the atmosphere, into energy-rich fuels and chemicals. While extensive research into a wide range of CO_2-derived fuels, ranging from simple two-electron products such as carbon monoxide and formic acid to more complex molecules like methanol (CH_3OH) and multi-carbon products including ethanol (C_2H_5OH), ethylene (C_2H_4), ethane (C_2H_6) and acetic acid (CH_3COOH), the question of which product pathway offers the optimal balance of process efficiency, infrastructure compatibility and economic viability remains an open question. This ongoing ambiguity underscores the need for a nuanced evaluation of both thermodynamic and kinetic favorability and practical implementation across different fuel candidates.

Additionally, critical aspects such as the integration of efficient upstream CO_2 capture and downstream product separation are often overlooked, despite their significance to overall system viability and practical applicability. Moreover, as the research in this field advances, the standardisation of both research methodologies and characterisation techniques becomes paramount to ensure the accuracy and reproducibility of reported results for accurate reporting.

In this perspective, we examine the key challenges impeding the advancement of solar-driven CO_2RR and assess the progress of current technologies in establishing a viable solar fuels industry. Particular emphasis is placed on techno-economic factors that shape system feasibility, including STF, capital device costs and the market compatibility of CO_2-derived products. Drawing from this analysis, we highlight strategic directions for future research and innovation that could accelerate technological breakthroughs and facilitate the transition of CO_2RR systems from laboratory-scale demonstrations to commercially relevant applications. We aim to provide a framework for guiding the next phase of development in solar fuels, integrating both scientific and economic perspectives to identify realistic pathways toward sustainable implementation.

2. Challenges

2.1 Reaction barriers

Direct CO_2RR remains considerably more complex and technically demanding than water splitting, which is another important application in the field of artificial photosynthesis. Fuel production through this pathway typically requires the concurrent evolution of molecular oxygen, which is released into the atmosphere and later acts as an oxidising agent during fuel utilisation.[14] This reaction with the reduced fuel regenerates the original reactants, thereby completing a carbon-neutral cycle. Nevertheless, the activation of CO_2 and H_2O to generate energy-rich fuels poses substantial thermodynamic and kinetic barriers.

These transformations are inherently endothermic processes, with Gibbs free energy requirements exceeding that of water splitting, particularly for the formation of methane, methanol and multi-carbon compounds (Table 1). Additionally, CO_2RR faces a high energy penalty as a consequence of the high dissociation energy of the C=O bonds (approximately 750 kJ mol^{-1}),[15] which requires considerable energy input for activation. In addition to the activation barrier of CO_2, CO_2RR pathways consist of multiple single steps, each contributing to the overall kinetic sluggishness of the reaction. The overall conversion process entails complex reaction pathways involving bond-breaking and bond-forming steps, coupled with multi-electron and proton transfer mechanisms.

In practice, the energy input required for CO_2RR is even greater than the thermodynamic minimum. To drive the electrochemical CO_2RR at appreciable reaction rates, an overpotential of approximately 1.0 V beyond the thermodynamic requirement is typically necessary.[17] Bias-free photo(electro) chemical CO_2RR continues to suffer from low STFs primarily due to the limited photovoltages provided by semiconductor

Table 1 Comparison of thermodynamic ($\Delta G°$ and $E°_{cell}$) and kinetic barriers (the number of electrons involved) for representative CO_2RR pathways coupled with water oxidation

Product	Overall reaction	$\Delta G°$ (kJ mol^{-1})[a]	$E°_{cell}$ (V)[a]	Half-reaction	$E°_{cathode}$ (V)[b] (ref. 16)
Hydrogen (H_2)	$H_2O(l) \rightarrow H_2(g) + \frac{1}{2}O_2(g)$	237.13	1.23	$2H^+ + 2e^- \rightarrow H_2$	−0.41
Carbon monoxide (CO)	$CO_2(g) \rightarrow CO(g) + \frac{1}{2}O_2(g)$	257.19	1.33	$CO_2 + 2H^+ + 2e^- \rightarrow CO + H_2O$	−0.52
Formic acid (HCOOH)	$CO_2(g) + H_2O(l) \rightarrow HCOOH(l) + \frac{1}{2}O_2(g)$	270.14	1.40	$CO_2 + 2H^+ + 2e^- \rightarrow HCOOH$	−0.61
Methane (CH_4)	$CO_2(g) + 2H_2O(l) \rightarrow CH_4(g) + 2O_2(g)$	817.90	1.06	$CO_2 + 8H^+ + 8e^- \rightarrow CH_4 + 2H_2O$	−0.24
Methanol (CH_3OH)	$CO_2(g) + 2H_2O(l) \rightarrow CH_3OH(l) + \frac{3}{2}O_2(g)$	702.35	1.21	$CO_2 + 6H^+ + 6e^- \rightarrow CH_3OH + H_2O$	−0.38
Ethane (C_2H_6)	$2CO_2(g) + 3H_2O(l) \rightarrow C_2H_6(g) + \frac{7}{2}O_2(g)$	1467.35	1.09	$2CO_2 + 14H^+ + 14e^- \rightarrow C_2H_6 + 4H_2O$	−0.27
Ethylene (C_2H_4)	$2CO_2(g) + 2H_2O(l) \rightarrow C_2H_4(g) + 3O_2(g)$	1331.13	1.14	$2CO_2 + 12H^+ + 12e^- \rightarrow C_2H_4 + 4H_2O$	−0.35
Acetic acid (CH_3COOH)	$2CO_2(g) + 2H_2O(l) \rightarrow C_2H_4O_2(l) + 2O_2(g)$	873.08	1.13	$2CO_2 + 8H^+ + 8e^- \rightarrow C_2H_4O_2 + 2H_2O$	−0.30
Ethanol (CH_3CH_2OH)	$2CO_2(g) + 3H_2O(l) \rightarrow C_2H_5OH(l) + 3O_2(g)$	1325.45	1.15	$2CO_2 + 12H^+ + 12e^- \rightarrow C_2H_5OH + 3H_2O$	−0.33

[a] At standard conditions (1 atm, 298 K). [b] Versus a normal hydrogen electrode (NHE) at pH 7, 298 K, 1 atm gas pressure and 1 M for other solutes.

light absorbers, remaining a significant obstacle to its practical implementation.[18]

2.2 Selectivity

Beyond the thermodynamic and kinetic challenges described above, the complexity of CO_2RR is further increased by the wide range of possible reaction pathways and products. The multi-electron transfer processes involved can lead to the formation of various products through multiple intermediates, each with different degrees of reduction and associated energy demands. This inherent diversity introduces a second major obstacle in CO_2RR: achieving high selectivity toward a single, desired product. In practice, the CO_2RR often yields a diverse array of products with different carbon oxidation states, resulting in complex product mixtures. The involvement of proton donors further complicates the catalytic process, as protons can also be readily reduced to H_2, competing with CO_2RR. Selectivity is not only critical for maximising process efficiency but also for simplifying downstream separation and ensuring compatibility with existing energy and chemical infrastructures.

In photocatalytic CO_2RR, CO and formic acid are the most commonly observed products, primarily due to the limited photovoltage generated by typical photocatalyst materials, even when paired with an appropriate catalyst.[16] Metallic Ag nanoparticles represent a well-established example, favouring CO formation at low overpotentials *via* a straightforward two-electron pathway that generally proceeds through a single key intermediate.[19–21] This behavior is largely attributed to Ag's comparatively weak CO adsorption strength relative to Pt, which promotes rapid CO desorption and suppresses the competing hydrogen evolution reaction.[22] A representative photocatalyst is $ZnGa_2O_4$ loaded with metallic Ag nanoparticles, which drives CO_2RR coupled with water oxidation to produce CO and O_2 in an almost stoichiometric 2 : 1 molar ratio under UV irradiation, achieving CO selectivity as high as 95.0%.[23] Although Ag obtained by photodeposition, wet impregnation, or chemical reduction presents in the metallic state, the choice of deposition method exerts a significant influence on particle size and dispersion. In particular, chemical reduction yields highly dispersed Ag nanoparticles (~10 nm), dramatically smaller than those produced by photodeposition or impregnation (~100 nm). This reduced particle size and enhanced dispersion result in higher photocatalytic activity for CO_2-to-CO conversion. These results highlight the critical role of nanoscale structural control in optimising catalytic performance.

In contrast, electrochemical CO_2RR driven by solar cells at relatively high overpotentials can access a broader range of catalytic pathways. While this enables the formation of products beyond CO and formic acid, including methane, ethylene and more reduced liquid products such as ethanol, it often comes at the expense of selectivity.[24] Copper-based electrodes are particularly notable for their ability to form multi-carbon species. Reported products span C_1 (methane), C_2 (ethylene, acetaldehyde, ethanol) and even C_3 (propanol, propionaldehyde) species.[25] The activity and selectivity of Cu-based catalysts are dictated by fine control over their morphology

and electronic structure. Key structural parameters include particle size, shape, defect density, composition and oxidation state, which alters the coordination number of the active sites, local electronic structure by the presence of subsurface oxygen and re-adsorption of intermediates by the interparticle distance.[21,26] Reaction environment also exerts a decisive influence: solvent identity, pH, ionic composition, buffer strength and mass-transport dynamics collectively shape the CO_2RR pathway and, ultimately, the product distribution.[27,28] High efficiency and selectivity can only be achieved through the optimization of catalyst structure and composition, combined with the selection of the most favorable electrolyte environment.

The development of light-driven CO_2RR technologies has advanced far beyond the initial focus on metallic nanoparticles and metal oxides, now encompassing a diverse array of materials, including bimetallic alloys, metal sulfides and nitrides, MXenes, carbon-based metal-free catalysts and single-atom catalysts.[16,29–32] Inorganic catalyst architectures have attracted particular interest for their ability to precisely regulate charge separation and transport through targeted materials engineering strategies, such as controlled doping, defect tuning and heterojunction construction.[33,34] Their structural simplicity allows modular adaptation, and carefully optimised loading methods can fine-tune key physicochemical properties, including composition, oxidation state, crystal phase, particle size distribution, morphology, dimensionality and surface area, to enhance activity. The next research frontier lies in developing effective strategies to enhance the selectivity of multi-carbon products and suppress chemical and photoinduced degradation. Replacing noble-metal components with earth-abundant alternatives also remains a key objective.

Molecular catalysts offer an alternative approach, combining tunable active sites with the capability for *in situ* spectroscopic analysis of mechanistic pathways.[35,36] For example, transition-metal complexes, with multiple accessible redox states, can mediate multi-electron transfer and coordinate CO_2 in various binding modes, such as through the C=O double bond, the carbon atom alone, or the oxygen atom alone.[37–39] The transition-metal centre can then act as an inner-sphere electron-transfer agent, activating CO_2 for subsequent conversion. Compared with inorganic nanoparticles, molecular complexes often deliver higher selectivity, and their catalytic properties can be tailored through rational ligand and metal-centre design.[36] However, their application is often limited by reliance on homogeneous operation in organic solvents with added light absorbers, sacrificial donors and electron relays, making them incompatible with water as an electron source.[40] Immobilising these complexes on semiconductor photosensitisers offers a promising way to overcome such limitations: the semiconductor harvests light and transfers photogenerated electrons to the molecular catalyst on timescales suited to catalysis, enabling efficient and selective CO_2RR.[40] Nevertheless, even in aqueous systems producing monocarbons such as CO and HCOOH,[11,41] slow interfacial electron transfer remains a performance bottleneck.

Abiotic catalysts face fundamental constraints in selectively forming multi-carbon products from CO_2. Semi-artificial photosynthesis seeks to address this by integrating biocatalysts, including purified enzymes and whole cells, with semiconductors as light absorbers. While enzymes provide exceptional catalytic turnover rates and product selectivity, their activity is largely confined to natural metabolic pathways, restricting product formation mainly to CO and HCOOH.[42–44] They also face challenges in stability, integration with semiconductor interfaces and the requirement for direct electron transfer to avoid mediators or cofactors.

Microbial hybrid systems represent a promising alternative. Non-photosynthetic microorganisms can be endowed with specific CO_2 metabolic pathways, enabling the synthesis of target chemicals with high selectivity.[45–47] These organisms utilise activated carbon intermediates, such as acetyl-CoA, to drive C–C coupling without incurring the energetic penalties associated with reactant reactivation.[48] By pairing the high light-harvesting efficiency of semiconductors with the metabolic versatility, self-replication and self-repair capacity of whole-cell catalysts, bacteria–semiconductor hybrids combine the advantages of biological and inorganic systems. The main challenge is to precisely control and optimise the biotic–abiotic interface to maximise charge transfer and sustain catalytic performance.

Table 2 provides a comparative summary of the advantages and challenges of the different catalyst classes.

2.3 CO_2 source

Beyond reaction efficiency limitations, the nature of the CO_2 feedstock itself poses significant practical challenges for real-world implementation. CO_2 feedstocks for solar-driven CO_2RR systems can originate from a range of sources, each with distinct characteristics that influence system design and feasibility. Globally, ~45% of the anthropogenic CO_2 emissions come from fossil-fuel power plants (15 Gt CO_2 per year), and industrial processes such as cement production (~2 Gt CO_2 per year).[49]

Industrial flue gases typically contain CO_2 concentrations of 10–15% along with impurities such as oxygen, nitrogen oxides and sulfur oxides, which can degrade catalyst performance and require pre-treatment.[50] The separation energy for post-combustion capture from such point sources is typically 3.5–3.9 GJ per ton CO_2, with capture costs in the range of 30–60 USD per ton CO_2 for coal-fired plants and higher for more dilute industrial streams.[51]

Atmospheric CO_2, although widely distributed, exists at a much lower concentration (~0.04%), making its capture energy-intensive (~0.6–6.6 GJ ton^{-1} CO_2)[17] and best suited for net-negative emission strategies when paired with renewable energy.[52] Current direct air capture costs are estimated at 143–297 USD per ton CO_2, with projections as low as 22–77 USD per ton CO_2 by 2050.[53]

In parallel, amine-based capture systems, particularly those using monoethanolamine, have gained interest not only for

Table 2 Comparison of catalyst types for light-driven CO_2RR: main products, advantages and challenges

Catalyst types	Main products	Advantages	Challenges
Inorganic materials	Broad range (C_1, C_2 and C_3 products)	• Tunable charge separation and transport • Well-controlled physicochemical properties • Easy integration with substrates • High stability • High scalability	• Limited selectivity for multi-carbon products • Chemical and photoinduced corrosion • Maintaining long-term stability • Replacing noble metals with earth-abundant materials
Synthetic metal complexes	CO, HCOOH, *etc.*	• Tunable active sites and catalytic performance • High active site density • Suitable for *in situ* spectroscopic studies • High selectivity	• Limited operation in aqueous media • Chemical and photoinduced corrosion • Maintaining long-term stability • Efficient interfacial electron transfer • Multi-carbon products formation
Enzyme	CO, HCOOH, CH_3OH, *etc.*	• High active site density • High product selectivity • High catalytic turnover per active site	• Precise control of reaction kinetics and equilibrium • Fragile with poor stability • Limited capability for multi-carbon product formation • Efficient interfacial electron transfer • Difficult incorporation into substrate surfaces; complex interface control • Large-scale application limited by protein purification demands
Bacteria	CH_4, CH_3COOH, *etc.*	• Self-replication and self-repair • High product selectivity • Capable of multi-carbon product formation • Operation under ambient conditions • Potential for large-scale application	• Controlling and optimising the biotic–abiotic interface • Efficient interfacial electron transfer and mass transport • Susceptibility to poisoning by hybrid materials or products • Tailored CO_2 metabolic pathways for broad product synthesis • Regulatory and biosafety considerations

their capability in CO_2 absorption but also for their potential to enable direct (photo)electrochemical conversion of captured CO_2 without a separate desorption step.[54] Integration with industrial facilities, which can supply significant waste heat, offers the potential to offset much of the energy required for CO_2 capture and purification.

Considering these diverse feedstocks is essential for advancing realistic and scalable CO_2 utilisation technologies. In the near term, fossil point sources remain the most practical CO_2 supply for CO_2RR deployment, transitioning in the medium term toward biomass-derived CO_2 to reduce net emissions, and ultimately relying in the long term on net-negative resources such as direct air capture (DAC) to ensure a closed carbon cycle.

2.4 Product separation

While the development of solar fuel systems with high selectivity and STF remains a central focus of current research, we argue that practical considerations such as product purification, storage and transportation must also be integrated into system design. These downstream challenges are essential to address if CO_2RR technologies are to advance beyond the laboratory and into real-world applications. In practice, these considerations often weigh just as heavily as intrinsic catalytic performance in determining the economic feasibility of a technology, as purification and logistics can account for a substantial fraction of total system costs.

For instance, product separation is a deeply connected challenge in CO_2RR. Even in systems engineered for high

selectivity, the CO_2RR process often yields mixtures of products (water medium, unreacted CO_2, CO_2-derived fuel, supporting electrolyte, *etc.*), especially under practical operating conditions. This makes product separation an unavoidable and technically demanding step, yet it is often underemphasised in early-stage system design and performance evaluations. In addition, product distribution can fluctuate depending on operating conditions, catalyst degradation, or fluctuating light intensity in solar-driven systems, adding variability that complicates purification strategies.[28]

Unlike water splitting, which produces only H_2 and O_2 gases that are relatively easily separated from aqueous solution and from each other using molecular sieve membranes,[55] CO_2RR typically produces a range of gaseous and liquid products. The gas stream produced in CO_2RR may contain methane, ethylene and carbon monoxide, along with H_2 obtained from side reactions and unreacted CO_2, water vapour and carrier gases such as N_2 or Ar. In many cases, the partial pressures of these products are low, which necessitates additional compression steps prior to storage or transport. For example, pressurising a 50 mol% CH_4 mixture from 1 to 10 bar requires energy equivalent to 1.4–2.0% of CH_4's combustion enthalpy, increasing to 7–10% for a dilute 10 mol% CH_4 mixture. Pressure-swing adsorption (PSA) to remove CO_2 from 50% CH_4/50% CO_2 biogas can require ~15% of CH_4's combustion enthalpy, water scrubbing ~5% and cryogenic distillation 9.5–12%.[17] Meeting pipeline specifications typically requires reducing inert gases (CO_2, N_2) to below 4% and CO to <700 ppm, adding further purification complexity and cost.[17]

The liquid phase typically includes formate, acetate, methanol, ethanol and propanol in addition to unreacted water and dissolved electrolyte salts. Complete separation of these components from CO_2RR products presents a considerable challenge, requiring the separation of gas and liquid phases, the use of coalescers to remove condensable vapours from the gas stream, staged cryogenic distillation to isolate individual gaseous products, and the integration of pervaporation, distillation and membrane separation techniques to separate liquid-phase products.[17] For dilute liquid products, concentration before final purification is often necessary, which may involve multi-effect distillation, membrane-assisted evaporation, or hybrid separation systems to reduce thermal energy consumption. For instance, separating a 10 wt% ethanol/water mixture by distillation requires energy equivalent to 12.6% of ethanol's combustion enthalpy, while a 1 wt% solution requires 146%.[17]

These separations require energy, potentially negating the energy benefits of using sunlight to produce high-energy-density products from CO_2. The energy requirements for product separation, along with the energy associated with CO_2 capture and the embodied energy of the equipment, are suggested to collectively remain below ~50% of the product's enthalpy of combustion.[17] This constraint is critical for maintaining a net-positive energy balance. It also helps justify the viability of CO_2RR processes for practical fuel production. Failure to meet this threshold could render the process energetically counterproductive, regardless of improvements in catalytic efficiency. Even at 100% selectivity toward a desired product, the intrinsic characteristics of many liquid products, such as the formation of azeotropes with water or high water solubility, pose significant challenges for efficient separation, especially at small production scales where economies of scale are not yet realised. This is particularly relevant for alcohols such as ethanol, which form azeotropes requiring energy-intensive separation steps, or for formic acid, where strong hydrogen bonding with water limits the applicability of simple distillation. In contrast, gaseous products such as carbon monoxide, methane, or ethylene benefit from higher partial pressures and physical-phase separation, making their recovery more straightforward and energetically favourable.[56] Nevertheless, the downstream purification remains necessary to meet fuel- or chemical-grade specifications, which carry significant compression or liquefaction energy penalties. An alternative strategy is to design offtaker processes with higher impurity tolerance, or ideally, systems capable of directly utilising the CO_2RR product stream "as produced," thereby reducing or eliminating certain purification steps and improving overall energy efficiency.

2.5 Stability and scalability

Significant advancements have been demonstrated in solar hydrogen production *via* water splitting, with successful demonstrations stably for about 1 year at scales up to 100 m^2.[55] In contrast, comparable progress for solar-driven CO_2RR remains unrealised. Bench-scale investigations are the norm, with PV–EC and PEC devices typically operating on the order of ~1 cm^2, and photocatalytic systems generally limited to areas ranging from a few square centimetres to several tens of square centimetres. Although certain electrocatalysts for CO_2RR, such as Ag and Sn, have been reported to maintain stable performance for more than 100 hours and, in some cases, several thousand hours,[57,58] demonstrated CO_2 and water conversion systems that rely solely on solar energy typically exhibit operational lifetimes limited to only several hours.

A representative demonstration of a relatively large-scale demonstration is a PV–EC system comprising five anode–cathode pairs, each with an electrode area of approximately 1000 cm^2.[59] The anodes are functionalized with IrO_x, while the cathodes are modified with a ruthenium-complex polymer supported on carbon, with all electrode pairs electrically connected in parallel. These electrochemical cells are integrated with six single-crystalline silicon photovoltaic cells of comparable size, connected in series. The system achieved an STF of 7.2% for the solar-driven CO_2RR to formate and maintained stable performance over a continuous operational period of three hours under one sun solar irradiation (AM 1.5G, 100 mW cm^{-2}). Another scale-up effort involves a photocatalyst sheet with an irradiation area of approximately 20 cm^2, integrating phosphonated Co(II) bis(terpyridine)-modified $SrTiO_3$:La,Rh and RuO_2/$BiVO_4$:Mo photocatalysts anchored on a gold layer, which attains an STF of 0.07% for CO_2-to-formate conversion during continuous operation over six hours.[11] In the EIC Horizon Prize "Fuel from the Sun" demonstration, a 10 cm^2 perovskite solar cell was integrated with a $BiVO_4$ photoanode and a selective $Cu_{92}In_8$ alloy CO_2RR catalyst to achieve unassisted water and CO_2 conversion to produce syngas (mixture of

CO and H_2) over 36 hours.[60] To demonstrate the modularity and scalability of this approach, a 0.7 × 0.5 m^2 reactor comprising a 10 × 10 array of these artificial leaves was deployed and benchmarked during a three-day outdoor performance test.

Based on comparisons among various solar-driven artificial photosynthetic systems,[3,61] photocatalytic systems are generally considered more favourable for scale-up, both from economic and performance standpoints. Their photocatalytic performance can be largely retained with increasing operating size, as pH gradients and IR drops are minimised by the close spatial coupling of the reduction and oxidation reactions. Moreover, the absence of a need for buffers or additional electrolytes reduces material and operational costs, while addressing critical scale-up challenges. In contrast, PV–EC and PEC systems face pronounced challenges during scale-up. The large-area cell commonly underperforms relative to the bench-scale counterpart across all major performance metrics, a trend largely attributed to challenges in ensuring uniform fabrication of photoelectrodes and catalysts, along with inherent limitations in mass transport.[62] Additionally, scale-up introduces increased series resistance and reduced charge carrier collection efficiency due to longer electron and hole transport pathways, especially in planar configurations, resulting in significant ohmic losses and voltage drops across the device.[63] Such issues may be mitigated through rational system design strategies that minimise the spatial separation between redox sites, reduce in-plane resistive losses,[64,65] and ensure uniform compression and fluid flow across the electrode area.[66]

2.6 Reliability of reporting the performance

In recent decades, significant progress has been made and numerous studies have been published in the field of solar-driven CO_2RR. However, it is crucial to realise that some reported CO_2RR performances have been measured under arbitrary, unverifiable and impractical conditions, thereby limiting their reliability and relevance. Several critical issues contributing to this problem are outlined below.

Reaction conditions. The nature of the reactants, including pH, the identity and concentration of ionic species and buffering strength as well as CO_2 flow rate, operation temperature and pressure, detailed information about the light source information (types, intensity and spectrum), significantly affect both the activity and selectivity of CO_2RR. These parameters, along with the active device area and the duration of operation, must be clearly reported alongside performance metrics to ensure reproducibility and meaningful comparisons.

Oxidation mechanism. As CO_2RR is a reduction process driven by photoexcited electrons, any system must incorporate an oxidation reaction to consume photogenerated holes. This oxidation half-reaction must be explicitly discussed along with the CO_2RR. In systems using water as the sole electron donor without the aid of sacrificial reagents, the formation of both CO_2RR products and water oxidation product (generally O_2) in a stoichiometric ratio is expected. Reports that present only CO_2RR products without confirming O_2 evolution raise concerns about the reaction mechanism, casting doubt on whether the observed activity truly results from a solar-driven reaction involving only CO_2 and water, or whether additional processes are contributing or some products remain undetected.

Production rate. In photocatalytic systems, the product evolution rate is frequently reported as a measure of photocatalytic activity. Although some studies have clearly emphasised that normalising the reaction rate by the mass of photocatalyst (*e.g.*, μmol g^{-1}) is fundamentally flawed and should be avoided,[67–69] this unit is still commonly used, even for comparative analysis. It is important to note that the reaction rate does not always scale linearly with photocatalyst mass due to the light-shielding effect (Fig. 3a). Bench-scale photocatalytic tests typically employ photocatalyst quantities in the order of 10 mg to several hundred milligrams, well below the point at which a plateau in product formation rate is reached, often before the photocatalyst mass approaches 1 g. Therefore, such mass-based normalisation can lead to misleading conclusions. It is recommended to report on the relationship between photocatalyst amount and product evolution rate, and to base performance comparisons on the maximum observed photocatalytic activity, as shown in Fig. 3a. In addition, normalising the reaction rate by surface area or active site density is also of limited validity, as photocatalytic performance is not solely governed by surface catalytic reactions. Instead, it is strongly influenced by bulk physical processes, including charge

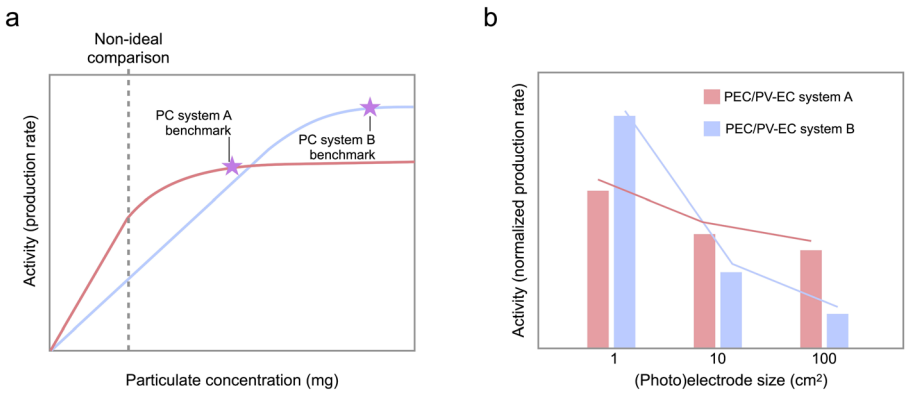

Fig. 3 Reliable comparison of different systems. (a) Relationship between photocatalyst mass and photocatalytic performance in particulate PC systems. (b) Variation in (photo)electrochemical performance with the active area of the samples in PEC and PV–EC systems.

generation, separation and transport within the photocatalyst. Therefore, such normalisation approaches may not accurately reflect the true photocatalytic efficiency or enable meaningful comparison across different materials and systems.[67]

Similarly, in PEC or PV–EC systems, the (photo)electrode size plays a critical role in determining observed performance metrics. The product formation rate and efficiency often deteriorate with increased device area due to increased series resistance, non-uniform current distribution and longer charge carrier transport distances.[63] Therefore, performance should always be compared at the same device scale to avoid overestimating scalability. As shown in Fig. 3b, system A exhibits inherently higher scalability than system B, maintaining more stable activity upon upscaling, although its performance at smaller scales is worse than that of system B.

STF and quantum efficiency. As the product formation rate in photocatalytic systems is influenced by numerous factors, including the light source, reaction temperature and pressure as well as reactor design, it is recommended to use STF and quantum efficiency as more rigorous and comparable performance metrics, provided that each system is evaluated under its respective optimal conditions. However, inaccuracies often arise when sacrificial reagents or external bias are employed during the reaction, yet the STF is calculated based on the standard Gibbs free energy changes (ΔG°) for the full conversion of CO_2 and water, as listed in Table 1. When sacrificial reagents are used for either CO_2RR or water oxidation, the reaction deviates from the full CO_2 and water conversion. Consequently, the corresponding ΔG° value differs dramatically, often being significantly lower and in some cases even negative.[70] For instance, the ΔG° for water splitting is +237.13 kJ mol^{-1}, whereas employing methanol as the electron donor for hydrogen production while concurrently releasing CO_2 ($CH_3OH(l) + H_2O(l) \rightarrow CO_2(g) + 3H_2(g)$), requires significantly less energy, with a ΔG° of only +9.04 kJ mol^{-1}. Therefore, STF should be calculated using the appropriate ΔG° for the actual reaction occurring in the system. Similarly, in PEC or PV–EC systems operating with an external bias, the electrical energy input must be accounted for in the STF evaluation to avoid overestimating the STF of the systems. In addition, when the testing conditions deviate from standard conditions (1 atm, 298 K), the values of ΔG° and standard cell potential (E°_{cell}) differ from those listed in Table 1 and must be recalculated accordingly. Regarding quantum efficiency calculations, it is incorrect to rely on normalised production rates (mol g^{-1} h^{-1}), particularly when monochromatic light sources are used, as the incident light intensity is often very low. Accurate reporting should be based on the actual production rates under specific measurement conditions to ensure meaningful comparisons.

Isotopic labelling experiment. As carbon is ubiquitous in the laboratory environment, both on sample surfaces and in reagents, it is essential to confirm the origin of CO_2RR products through isotopic labelling experiments. Such validation is particularly critical when organic compounds, such as alcohols, triethanolamine or cysteine, are employed as electron donors or when CO_2 captured in monoethanolamine solutions is directly utilised as a reactant.[50] In addition, a series of control experiments conducted in the absence of light irradiation and/or (photo)catalysts is essential to verify that the observed reactions are indeed driven by solar energy and proceed *via* a catalytic pathway.

Stability. We would like to emphasise that catalyst stability should be clearly distinguished from overall system stability. In several reported demonstrations, long-term operation is achieved not solely due to the intrinsic durability of the catalyst, but rather through external interventions such as periodic replacement of the electrolyte, membrane or other system components. While such measures can prolong functional operation, they do not reflect true catalyst stability. Therefore, it is critical that these operational conditions are transparently reported and clearly stated when evaluating or comparing long-term performance.

3. Product analysis

Global fuel consumption is currently dominated by natural gas (primarily methane, CH_4), diesel (a mixture of C_{10}–C_{15} saturated hydrocarbons, typically approximated by dodecane), jet fuel and kerosene and gasoline (composed mainly of C_4–C_{12} saturated hydrocarbons, often represented by octane) along with aromatic compounds such as benzene, toluene and xylenes (C_6–C_8).[17] While replacing these fossil-derived fuels with CO_2RR products would offer a substantial global impact and market relevance, a significant gap remains between the fuels that dominate current energy demand and those that can be accessed through established solar-driven CO_2RR pathways using state-of-the-art systems. Surveying the current progress in light-driven CO_2RR, the most commonly reported CO_2RR products are primarily C_1–C_2 compounds, including carbon monoxide, formic acid, methane, methanol, ethane, ethylene, acetic acid and ethanol, with the formation of C_3 or higher hydrocarbons remaining rare and challenging under current catalytic conditions.

3.1 Thermodynamic and kinetic barriers

Thermodynamic analysis provides the energetic framework within which CO_2RR pathways compete. When these reactions are formulated using water as the reductant (electron/proton source) and oxygen as the oxidation product, the associated ΔG° span a broad range: the formation of CO or formic acid involves relatively modest ΔG° value, whereas the synthesis of C_2 products (*e.g.*, ethanol, ethylene, ethane) requires significantly higher energies, with ΔG° values exceeding 1000 kJ mol^{-1}. However, in electro(photo)chemical systems, the more relevant thermodynamic parameter is the standard cell potential (E°_{cell}), derived from the relationship $\Delta G^\circ = -nFE^\circ_{cell}$, where n is the number of electrons transferred and F is the Faraday constant. When normalised by n, these large differences in ΔG° converge into a narrower range of standard potentials, falling within ~1.0–1.4 V, as summarised in Table 1.

Nonetheless, in practice, product selectivity is more strongly governed by kinetic barriers and the overpotentials required to activate competing multi-electron and multi-proton transfer

pathways.[16] These kinetic barriers correlate with the number of electrons involved in the product formation. As summarised in Table 1, the electron requirements increase in the following order: $H_2 = CO = HCOOH < CH_3OH < CH_4 = CH_3COOH < C_2H_4 = CH_3CH_2OH < C_2H_6$.

At the lower end of the trend, hydrogen evolution from water and CO_2RR to simple C_1 products, such as carbon monoxide and formic acid, are comparatively facile, as these reactions involve only two electrons and two protons, minimal bond rearrangements and relatively few intermediate species. These attributes make them the most accessible products, particularly in photocatalytic systems where the inherently low photovoltage and limited charge separation efficiency impose additional constraints on reaction pathways.[22] Under such conditions, product distribution is biased toward thermodynamically and kinetically favourable transformations.

As target products become progressively more reduced, the kinetic difficulty intensifies due to the increased number of electrons and proton-coupled electron transfer steps required. For instance, the formation of methanol, methane, acetic acid, ethylene, ethanol and ethane necessitates 6, 8, 8, 12, 12 and 14 electrons and protons, respectively. These complex and multi-electron pathways involve a broad range of intermediate species and intricate bond rearrangements, demanding precise control over reaction sequences, effective stabilisation of transient intermediates and finely tuned proton-electron transfer kinetics. Consequently, the selective and efficient production of such hydrocarbons and oxygenates hinges on the development of advanced catalytic architectures and carefully optimised reaction environments.[24,28]

In comparison, water splitting exhibits a standard cell potential E°_{cell} of 1.23 V, which is comparable to most CO_2RR pathways. Therefore, in aqueous systems, hydrogen evolution reaction often competes with CO_2RR, particularly under conditions or with catalysts that promote rapid proton reduction. This competition, combined with the inherently low solubility of CO_2 in water, presents a significant barrier to achieving high selectivity toward carbon-based products in CO_2RR.[71]

3.2 Market size

The relative current global market demand for common CO_2RR products generally follows this order (Table 3): $HCOOH < CO < CH_3COOH < C_2H_6 < CH_3OH <$ syngas $< CH_3CH_2OH < CH_4 < C_2H_4 < H_2$.

Formic acid currently occupies a relatively small segment of the global chemical market, primarily utilised in the leather and textile industries as a tanning agent and pH regulator.[72,73] Its application in cleaning products, notably for rust removal and descaling, is rapidly expanding, significantly contributing to market growth. The fastest expansion, however, is observed in the animal feed sector, driven by increasing global demand for meat and animal-derived products, particularly in developing regions, where formic acid acts as a preservative and antimicrobial additive.

Carbon monoxide similarly holds a limited standalone market, segmented into niche industrial applications such as metal fabrication, chemical synthesis, ore processing, pharmaceuticals and electronics.[74] However, CO's industrial value rises significantly when combined with hydrogen to form synthesis gas (syngas), a key intermediate for producing methanol, fuels, fertilisers and synthetic materials.[75] In the Fischer–Tropsch process, syngas is catalytically converted into liquid hydrocarbons that can serve directly as fuels or as feedstocks for conventional petrochemical manufacturing.[76]

Ethane and acetic acid possess moderately larger markets. Ethane is predominantly used for ethylene synthesis, acetic acid synthesis and as a refrigerant.[77] Acetic acid serves as a key feedstock for manufacturing chemicals such as vinyl acetate monomer, acetic anhydride and acetate esters, extensively employed in adhesives, coatings and textiles.[78]

Methanol's market is diverse, spanning construction, automotive and electronics, among other sectors.[79] The construction segment is projected to dominate, given methanol's use in producing foams, adhesives, plywood subfloors and plastics. Additionally, shifting fuel industries towards methanol and methanol-blended fuels, in response to environmental

Table 3 Economic assessment of common products from solar-driven CO_2RR

Product	Market size (USD)	Current price (USD per kg)	Production capacity (metric tons per year)	Allowable device price at STF of 10% (USD per m^2)
Hydrogen (H_2)	242.7 billion (2023)[86]	~1.39 (ref. 5)	97 (ref. 87)	187 (target price 3.5 USD per kg for green H_2)[88]
Carbon monoxide (CO)	3.36 billion (2023)[74]	0.20 (ref. 89)	~150 million (ref. 89)	138
Syngas	58.16 billion (2024)[90]	~0.2 (ref. 91)	246.18 million N m^3 h^{-1} (ref. 92)	159 (assuming H_2/CO ratio 2 : 1, target price ~0.6 USD per kg for renewable syngas)[93]
Formic acid (HCOOH)	2.11 billion (2023)[73]	0.66 (ref. 89)	1 million (ref. 89)	712
Methane (CH_4)	95.4 billion (2023)[82]	0.16 (ref. 89)	250 million (ref. 89)	20
Methanol (CH_3OH)	31.26 billion (2024)[79]	0.37 (ref. 89)	80.5 million (ref. 89)	107
Ethane (C_2H_6)	14.43 billion (2023)[77]	0.28 (ref. 94)	~80 million (ref. 94)	43
Ethylene (C_2H_4)	196.2 billion (2023)[84]	0.90 (ref. 95)	226 million (ref. 95)	120
Acetic acid (CH_3COOH)	13.80 billion (2024)[78]	~0.50 (ref. 96)	17.48 million (ref. 97)	218
Ethanol (CH_3CH_2OH)	77.12 billion (2023)[80]	0.51 (ref. 89)	77 million (ref. 89)	137

concerns associated with heavy fossil fuels, is anticipated to further propel market growth.

The transportation industry represents the dominant consumer of ethanol globally, driven primarily by increasing demand for renewable fuels.[80] This growth is largely attributed to supportive government policies, such as the Renewable Fuel Standards in the United States, EU directives and blending mandates in emerging economies, including Thailand, India and Brazil.[80] In the chemical sector, ethanol plays a crucial role as a raw material in the synthesis of compounds such as ethylene, acetic acid and ethyl acetate, which are essential for producing plastics, solvents, coatings and pharmaceutical ingredients. The shift toward greener, bio-based alternatives to fossil-derived chemicals, supported by favourable policy incentives, is expected to significantly expand ethanol usage in this area during the coming years.[81]

Methane, the primary constituent of natural gas, plays a critical role in the global energy landscape, with widespread application in electricity generation, residential and industrial heating, and as a fundamental feedstock in chemical synthesis.[82] Its versatility extends to specialised uses such as liquefied natural gas and liquid methane-based rocket fuels. In addition, ultra-high-purity methane is indispensable for the synthesis of graphene, a key material in the fabrication of microchips and transistors, which are crucial to almost all modern electronic devices. This expanding demand from the electronics sector is a significant driver of methane's market growth.

Among the various CO_2RR products, ethylene stands out as one of the highest-volume industrial chemicals, with its market expanding notably over the past decade. This growth is primarily driven by escalating demand for plastics, packaging and automotive components, alongside rapid developments in the construction and infrastructure sectors.[83,84] The market outlook remains positive, supported by ongoing trends in global population growth, urbanisation and industrial expansion. Ethylene's utility spans a broad spectrum of industries. The packaging sector constitutes the largest consumer segment, where ethylene is employed in the manufacture of films, containers and bottles. In the construction industry, ethylene derivatives are used in the production of pipes, fittings and insulation materials. The automotive sector utilises ethylene-based polymers in fabricating dashboards, bumpers and interior panels. Moreover, in the textile industry, ethylene serves as a precursor for the synthesis of synthetic fibers, thereby reinforcing its strategic importance across multiple manufacturing domains.

Finally, hydrogen holds the largest market demand among these chemicals, extensively utilised across various sectors, including chemical production (*e.g.*, ammonia synthesis), petroleum refining, metal processing and increasingly as a clean-energy carrier.[85,86] Recent growth in hydrogen consumption is primarily driven by the global push for cleaner fuels and the hydrogen market is expected to experience substantial expansion. Favourable regulatory frameworks and mounting environmental concerns continue to accelerate the development of hydrogen generation and utilisation technologies. Within this landscape, the ammonia production segment currently dominates, accounting for over 23.56% of the total market revenue in 2024.[85] Ammonia's potential to function as a carbon-free fuel, hydrogen storage medium and energy carrier further underscores the strategic significance of advancing renewable hydrogen technologies on a global scale.

3.3 Market price and production capacity

The economic viability of CO_2RR products is fundamentally shaped by two interrelated factors: market price and production capacity. While the former is influenced by demand-supply dynamics, production complexity, purity requirements, downstream applications and product applications, the latter is constrained by technological maturity, infrastructure readiness and raw material availability. There exists a substantial disconnect between high-value, low-volume products and those that are inexpensive yet industrially abundant. The general market price hierarchy of CO_2RR products and H_2, follows the trend (Table 3): CH_4 < syngas ≈ CO < C_2H_6 < CH_3OH < CH_3COOH ≈ CH_3CH_2OH < HCOOH < C_2H_4 < H_2. Conversely, the production capacity hierarchy tends to mirror this trend inversely, except C_2H_4 (Table 3): H_2 << HCOOH < CH_3COOH < CH_3CH_2OH < CH_3OH ≈ C_2H_6 < CO < C_2H_4 < syngas < CH_4.

Methane, which is the least expensive among CO_2RR products, dominates production capacity due to its extensive role as a primary energy carrier in global natural gas infrastructure. Its abundant natural reserves, highly developed global infrastructure and large-scale industrial production contribute to its economic accessibility and high scalability. Similarly, carbon monoxide and ethane are moderately priced and produced in relatively large quantities due to their availability as by-products in petrochemical processes. These compounds benefit from being integral to existing industrial value chains, albeit offering limited profitability as stand-alone CO_2RR targets. Syngas is among the less expensive products on the list, with a market price comparable to that of pure carbon monoxide and lower than that of pure hydrogen. This cost advantage primarily stems from its role as an intermediate in large-scale industrial processes such as steam methane reforming and coal gasification, where it is produced at high volumes. In contrast, the additional separation and purification steps required to obtain pure hydrogen introduce substantial energy demands and infrastructure costs, which significantly increase their market prices.[93,98]

Methanol and ethanol occupy a mid-tier position in both price and production capacity. Their wide-ranging applications in transportation fuels, solvents and chemical synthesis, along with partially developed renewable production pathways, render them promising CO_2RR products from both an economic and technological standpoint. Their prices reflect moderate production complexity and strong industrial demand, though ethanol pricing may fluctuate based on feedstock availability and biofuel mandates.

In contrast, formic acid and acetic acid are relatively high-value CO_2RR products with more specialised and niche applications. Despite their versatility in chemical synthesis, textiles and agrochemicals, their global production volumes remain

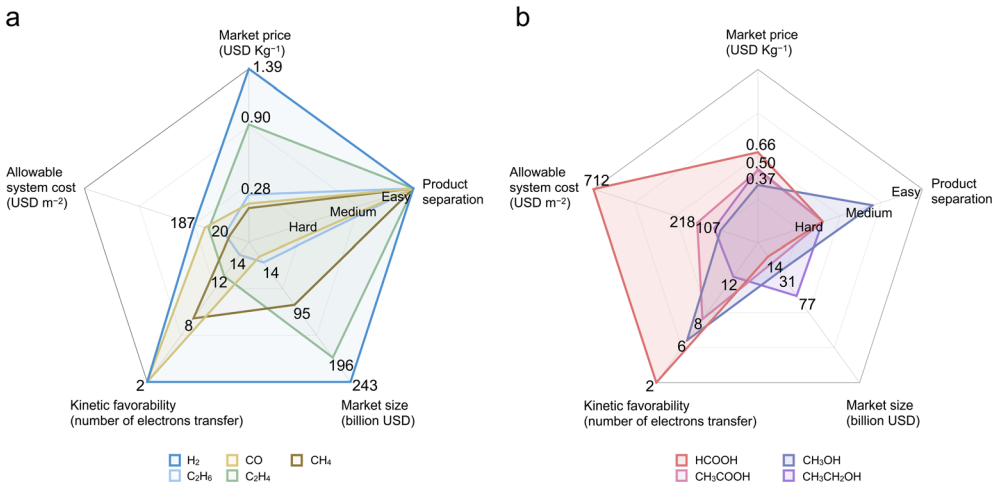

Fig. 4 Economic comparison of common products obtained from solar-driven CO_2RR. (a) Gaseous products and (b) liquid products.

comparatively modest. Formic acid, in particular, commands a higher market price due to its energy-intensive and technically complex production routes, such as the carbonylation of methanol.[73] Its use as a hydrogen carrier and antimicrobial agent in feed applications is growing, but these sectors have not yet driven large-scale production to match demand potential.

Ethylene represents a unique outlier among CO_2RR products. It is the only compound that combines both a high unit price and exceptionally high production volume. Its centrality in global manufacturing gives it robust and diverse demand, ensuring strong market value even at massive production scales. Given this dual advantage, C_2H_4 is a highly attractive target for CO_2RR, though it remains one of the most kinetically challenging products to produce selectively (Fig. 4a).

Green hydrogen, generated *via* electrolysis or photo(electro) catalytic processes driven by renewable energy, currently sits at the top of the pricing spectrum. The United States Department of Energy's goal of achieving a cost of 2.00–4.00 USD per kg for green H_2.[99] While hydrogen is already produced at an industrial scale, primarily through steam methane reforming, the overall global hydrogen output remains limited compared to carbon-based fuels. Moreover, green hydrogen accounts for only a small fraction of total hydrogen production, primarily due to the high cost and energy requirements of water electrolysis. The scalability of green hydrogen is further constrained by the underdeveloped infrastructure for its generation, compression and distribution.

3.4 System affordability

To quantitatively assess the interrelation among product market price, CO_2RR device capital cost and production efficiency, we employed the following equation:

$$\text{Product price} = \text{device cost/product amount.}$$

This formulation allows us to approximate the levelized product cost over the system's operational lifespan. The product yield can be correlated with the STF using the following equation:

$$\text{STF} = \frac{\text{output energy as fuels}}{\text{energy of incident light}} = \frac{(\text{mmol fuel s}^{-1}) \times (\Delta G\ \text{J mol}^{-1})}{(100\ \text{mW cm}^{-2}) \times (\text{area cm}^2)} \text{ at standard conditions}$$

Under the assumptions of standard one sun illumination (AM 1.5G, 100 mW cm^{-2}) for 6 hours per day, a projected service lifetime of 10 years and an annual capital depreciation rate of 5%, we derived the theoretical correlations among these variables. The resulting estimations are presented in Fig. 5.

Assuming an STF of 10% and referencing current product prices as summarised in Table 3, the allowable capital cost of CO_2RR and H_2 production systems follows the trend: CH_4 < C_2H_6 < CH_3OH < C_2H_4 < CH_3CH_2OH ≈ CO < syngas < H_2 < CH_3COOH << HCOOH.

Owing to the relatively low market prices of methane and ethane, the maximum allowable device cost for achieving economic viability for these products is constrained to below 50 USD per m^2, when STF is set as 10%. This imposes a considerable constraint, particularly when compared with the current cost structure of PV–EC systems. The high cost of PV–EC configurations, driven by the need for high-efficiency solar cells and electrocatalysts, robust corrosion–resistant components and precise integration of photovoltaic and electrochemical units, makes it difficult to meet this economic constraint under current manufacturing conditions. Even under current manufacturing conditions in China, solar cell modules still typically exceed 30 USD per m^2. Electrolysis components are also costly: for instance, anion exchange membranes are ~180 USD per m^2, while the electrocatalysts required for a cathode (Ag, 2 mg cm^{-2}) and an anode (IrO_x, 1 mg cm^{-2}) amount to approximately 1752 USD per m^2 in total.[100] Under optimistic scenarios, for example, increasing STF to 60%, the allowable device cost for methane production would only rise to approximately 120 USD per m^2, which still remains technologically and economically demanding with present manufacturing capabilities. A similar constraint applies to syngas, given its low market

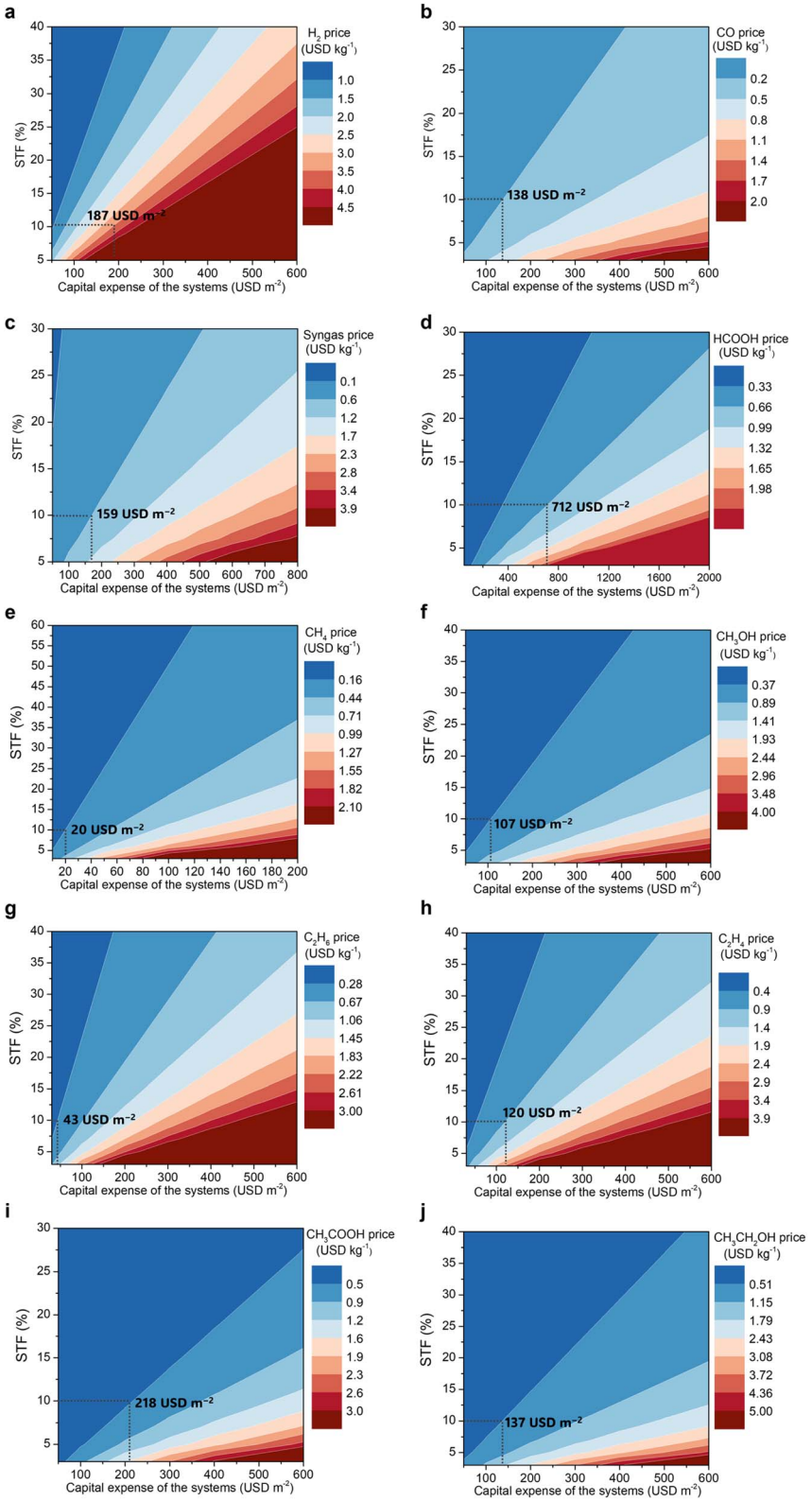

Fig. 5 Contour plots of the attenable price of (a) hydrogen (H_2) and various CO_2RR products: (b) carbon monoxide (CO), (c) syngas (H_2/CO = 2), (d) formic acid (HCOOH), (e) methane (CH_4), (f) methanol (CH_3OH), (g) ethane (C_2H_6), (h) ethylene (C_2H_4), (i) acetic acid (CH_3COOH) and (j) ethanol (CH_3CH_2OH) as a function of STF and capital expense for the system.

price. However, if a target price of ~0.6 USD per kg is considered for renewable syngas produced from circular carbon feedstocks,[93] the allowable capital cost could increase to 159 USD per m^2, assuming an H_2 to CO ratio of 2, which is typical for large-scale synthesis-gas-based production of chemicals such as methanol and dimethyl ether.[98,101]

Furthermore, the substitution of CO_2RR-derived fuels for fossil-based products with inherently low global demand does not offer a scalable or impactful solution to global CO_2 mitigation. Such limited-market substitutions are unlikely to exert a meaningful influence on global commodity prices either. Consider that at an STF of 10%, the theoretical annual methane yield is ~120 kg m^{-2}. Given the global methane production capacity of ~250 million metric tons per year, replacing just 10% of this volume *via* solar CO_2RR would necessitate the deployment of more than 200 km^2 of active reactor surface. This spatial requirement, coupled with economic and technological constraints, suggests that solar-driven CO_2-to-CH_4 conversion is unlikely to achieve cost-competitive parity with conventional methane production in the foreseeable future.

For mid-value CO_2RR products such as methanol, ethylene, ethanol and carbon monoxide, the estimated allowable device cost to achieve economic parity with current market prices ranges from approximately 100 to 140 USD per m^2, assuming an STF of 10%. While this cost window is less stringent than that associated with lower-value products like methane and ethane, it still presents substantial economic hurdles for PV–EC systems. Realistically, achieving STF values in the range of 20–30% would be required to accommodate higher device costs on the order of 200 to 400 USD per m^2, which could enable commercial viability if relatively expensive electrocatalysts are used. By contrast, photocatalytic panel systems that use lower-cost semiconductors than crystalline silicon, such as oxide materials (*e.g.*, $SrTiO_3$ and $BiVO_4$) and compatible with scalable, cost-efficient fabrication techniques (*e.g.*, screen printing),[102] present a promising alternative.[3,4] These systems avoid the integration complexities and cost burdens associated with coupling high-efficiency photovoltaic modules to electrochemical reactors. If implemented at commercially relevant scales, such systems may provide a more pragmatic route to economically competitive production of mid-value CO_2-derived fuels and chemicals. The PEC configuration integrates light absorbers, ionic membranes and electrocatalysts within a single reactor, thereby reducing the number of components, simplifying system architecture and enabling potentially greater operational flexibility. Despite these advantages, techno-economic analyses indicate that the economic competitiveness of PEC systems remains constrained by material costs, device design and limitations in manufacturing scale.[5,100] The highest-performing PEC devices reported to date still depend on photovoltaic-grade semiconductors with buried junctions, which are expensive to fabricate.[103,104] Achieving economic viability is suggested to require a combination of strategies, such as the use of concentrated solar irradiation, lowering material costs, operating under pressurised conditions and substantially reducing CO_2 capture costs.[100]

Formic acid and acetic acid appear to be among the most promising target products for current solar-powered CO_2RR technologies, primarily due to the combination of their relatively high market prices and modest global production volumes. These factors translate into more favourable economics for early-stage CO_2RR deployment. More broadly, the juxtaposition of market price and production capacity underscores a fundamental dilemma in chemical product development: products that are economically attractive due to their high market value often present substantial challenges to large-scale synthesis, such as the current formic acid product. Within this context, formic acid and acetic acid represent a rare convergence of economic viability and moderate production scale, positioning them as compelling near-term candidates for the deployment of solar-driven CO_2RR technologies under realistic techno-economic constraints. Assuming an STF of 10%, a square meter of the CO_2RR device could theoretically produce about 1 kg of formic acid annually. Given the current global production capacity of formic acid, around 1 million metric tons per year, reaching 50% of this value through CO_2RR would require ~500 000 m^2 of active solar reactor area. While this scale is not trivial, it is considerably more attainable than what would be required for methane. Large-scale deployment of CO_2RR for these chemicals could potentially saturate or reshape their global supply chains, resulting in a tangible impact on market structure and carbon mitigation efforts.

3.5 Separation

Generally, gaseous products such as carbon monoxide, methane, ethane and ethylene are considerably easier to separate from the reaction medium compared to liquid products. Their low solubility in water, high volatility and distinct phase from the aqueous electrolyte allow for efficient recovery.[105,106] In contrast, liquid CO_2RR products, such as formic acid, methanol, ethanol and acetic acid, are all highly soluble in water and typically generated alongside aqueous electrolytes, making their separation both technically demanding and energy-intensive.

In a simplified scenario where only the target liquid product coexists with water and dissolved salts, separation remains nontrivial due to azeotrope formation and similar volatilities. Formic acid forms strong hydrogen bonds with water and exhibits azeotropic behaviour, limiting the effectiveness of simple distillation and often requiring energy-intensive methods such as reactive distillation, membrane separation or solvent extraction.[107] Ethanol, widely known for forming a minimum-boiling azeotrope with water, demands extractive distillation or molecular sieves for purification. Acetic acid, although less volatile than alcohols and partially dissociated in aqueous media, presents challenges due to its strong hydrophilicity and corrosive nature, often requiring liquid–liquid extraction with specialised solvents, sometimes followed by distillation or pervaporation.[108] Among these, methanol is generally considered relatively easy to separate under high-concentration conditions due to its relatively low boiling point and favourable volatility, which allow for effective recovery by conventional distillation.

While gaseous CO_2RR products are inherently easier to isolate and scale, the separation of liquid products remains a critical bottleneck, particularly at low product concentrations. Tailoring system designs to favour gas production or integrating *in situ* separation strategies[106,109] for liquid fuels will be essential to achieving practical and energy-efficient solar fuel production.

4. Future opportunities

Despite recent progress, huge challenges remain before practical deployment can be realised. The commercial feasibility of CO_2RR systems depends not only on achieving target STF and high selectivity toward the desired product but also on maintaining long-term device stability under operational conditions. Importantly, the resulting CO_2-derived fuels and chemicals must rival those produced by mature industrial processes in terms of lifecycle cost and energy consumption, as long-term competitiveness cannot rely solely on government subsidies or policy incentives for greener alternatives.

Overcoming these multifaceted challenges will require concerted progress across several domains. Advances in catalyst development must focus on enhancing activity, selectivity and robustness. Simultaneously, innovations in device architecture and reactor engineering are needed to improve light harvesting and mass transfer while minimising system costs. Furthermore, integration of these components into scalable modular systems, which are compatible with intermittent solar inputs, will be key to enabling widespread adoption.

To address these needs and advance the field toward commercial viability, we propose the following strategic directions.

4.1 Enhancing STF

Increasing STF is arguably the most pivotal metric in determining the viability of solar-powered CO_2RR technologies. For most commercially relevant CO_2RR products, including methanol, ethylene, ethanol and acetic acid, an STF exceeding 10% or even 20% is essential to approach economic competitiveness in the context of the allowable device costs derived from market price benchmarks (Fig. 5). Formic acid may be an exception, where lower STF thresholds (*e.g.*, ~5%) could still support viable deployment due to its high market value and relatively low global production volume. Nonetheless, even in such cases, higher STF values would substantially improve system economics and scalability.

Achieving high STF requires coordinated advancements across multiple fronts of material science and systems engineering. Key among these is a deeper mechanistic understanding of light absorption, charge separation and migration and catalytic surface reactions. Recent progress in microscopies and spectroscopic tools, such as surface photovoltage microscopy,[110] ultrafast transient absorption spectroscopy,[111] *operando* Fourier transform infrared spectroscopy and Raman spectroscopy,[112,113] has enabled real-time insights into catalyst changes, charge carrier dynamics and intermediate species. Such insights are critical for identifying unknown mechanisms and guiding the rational design of more efficient catalysts.

Simultaneous advances in computational chemistry, particularly density functional theory, have substantially improved our mechanistic understanding of CO_2RR, allowing for the elucidation of reaction energetics, identification of key intermediates and determination of active site characteristics.[114] Alongside these developments, machine learning and artificial intelligence (AI) have emerged as powerful tools for accelerating catalyst discovery and system optimisation.[115,116] Machine learning-assisted inverse design and high-throughput virtual screening have enabled the rapid identification of candidate materials with tailored optoelectronic properties.[117] Moreover, AI-driven platforms are increasingly utilised to streamline experimental workflows, reduce human labour and accelerate development cycles.

However, the effective and responsible application of these technologies requires careful consideration and close interdisciplinary collaboration between materials scientists, catalysis experts and machine learning specialists. Accurate prediction models hinge on access to large and high-quality datasets that are not only quantitatively robust but also curated with a deep understanding of the CO_2RR process. Unlike data derived from standard physicochemical measurements, catalytic activity and selectivity are influenced by multifactorial parameters, many of which are not consistently or explicitly reported in the literature. In the context of semiconductor-based photocatalysis, for instance, readily available descriptors such as bandgap are often overemphasised in the prediction, despite the fact that they primarily relate to light absorption. In contrast, crucial charge properties including carrier density, migration length and charge separation efficiency, as well as surface catalytic behaviours that dictate reaction kinetics and selectivity, are rarely reported or inadequately characterised. This paucity of comprehensive and standardised descriptors presents a major obstacle to the development of robust and data-driven predictive models.

Furthermore, we argue that models should not be evaluated solely by their ability to reproduce known results, but by their capacity to guide new, verifiable discoveries through scientifically meaningful correlations and predictive validity. Incorporating the digital and analytical tools into a closed-loop framework, where experimental data continuously inform computational models, which in turn generate predictive insights to guide subsequent experiments, has the potential to accelerate the discovery-to-deployment pipeline for CO_2RR technologies. Moreover, such integration holds the potential to uncover unconventional materials that simultaneously maximise photon utilisation, charge mobility and catalytic selectivity.

The integration of AI and computational tools should not replace domain expertise but rather augment it. The selection of features and training parameters must be grounded in a deep chemical and mechanistic understanding of CO_2RR processes. It is only through experimental insight, theoretical rigour and computational innovation that meaningful progress can be made toward the rational design of efficient, selective and stable materials and systems for solar-driven CO_2RR.

4.2 Reducing device cost

To achieve economically viable solar-driven CO_2RR, the system must meet specific cost thresholds associated with device fabrication, operation and installation. While efforts to lower the cost of materials and manufacturing are essential, it is equally important to address auxiliary cost factors, for example, land acquisition and usage, which constitute a substantial portion of the total system cost. Achieving appreciable production levels typically requires an extensive active area, often exceeding 1 km^2. This demand introduces a critical challenge: competition for land between residential development and food production. Consequently, siting CO_2RR facilities in non-urban settings, such as agricultural zones or desert environments (Fig. 6), would be a more practical strategy to reduce capital expenditure and complexity.

At first glance, deploying renewable energy systems in agricultural regions may seem counterproductive due to potential land-use conflicts with food production. However, the emergence of agrivoltaics, a dual-use strategy integrating photovoltaic technologies with crop cultivation, has demonstrated significant potential for optimising both energy generation and agricultural productivity.[118] Since many crops do not require the full solar spectrum or continuous direct sunlight irradiation, the installation of semi-transparent or spatially distributed panels can create beneficial microclimates by reducing evapotranspiration and providing partial shading, often enhancing crop yields. These systems not only generate additional revenue for farmers through electricity sales but also support decentralised power generation, reducing transmission losses and improving grid resilience. Solar-utilised CO_2RR systems may be co-located under similar configurations, further expanding land-use efficiency.

Desert regions, which account for approximately 33% of the Earth's land surface and are defined by an aridity index below 0.2, represent an underutilised opportunity for renewable energy deployment. These areas receive exceptionally high solar irradiation, typically ranging from 2000 to 2800 kWh per m^2 per year, nearly double that of temperate regions like London (~1000–1200 kWh m^{-2}),[119] making them especially attractive for solar fuels production due to significantly reduced payback times. The vast expanses of low-cost, sparsely inhabited land in rural deserts offer ideal conditions for large-scale energy projects, minimising land-use conflicts and simplifying regulatory approvals. Deserts are also suitable for hybrid energy systems, as solar resources can be complemented by wind energy, which often peaks when solar intensity is lower.

However, key challenges must be addressed to ensure feasibility. Water scarcity remains a significant barrier, as CO_2RR requires water as an electron donor. Innovations such as atmospheric water harvesting and moisture capture inspired by Namib beetles,[120] and metal–organic frameworks[121,122] offer promising solutions for localised water generation. Additionally, the harsh environmental conditions, including extreme temperatures, sandstorms and dust, necessitate robust design and automated maintenance systems. Dust mitigation and routine cleaning, potentially *via* automated systems, are essential to maintain operational efficiency.

Open water bodies, including oceans, seas and lakes, offer substantial potential for solar fuel generation through floating CO_2RR platforms. The deployment of floating technologies is garnering significant interest due to several advantages over land-based systems, such as higher solar irradiance exposure due to reduced shading, enhanced energy conversion efficiency *via* passive cooling from the surrounding water and the alleviation of land-use conflicts.[123,124] These systems are particularly attractive for island countries and remote coastal regions where land availability is limited but solar resources are abundant. Integrating such facilities with existing offshore infrastructure, including decommissioned oil rigs and artificial islands, could significantly reduce capital expenditure by utilising pre-existing platforms, while also revitalising remote economies through solar fuel production. Offshore locations also present unique opportunities for carbon capture and utilisation. The CO_2 captured from offshore carbon capture and storage units can serve as a feedstock for CO_2RR, aligning with circular carbon economy goals.

Nonetheless, the utilisation of CO_2RR systems in marine environments introduces several technical and environmental challenges. Chief among them is the need to maintain high performance for long-term operation under saline conditions. Seawater can degrade both devices and catalytic materials, necessitating the development of robust, corrosion–resistant systems and protective engineering strategies.

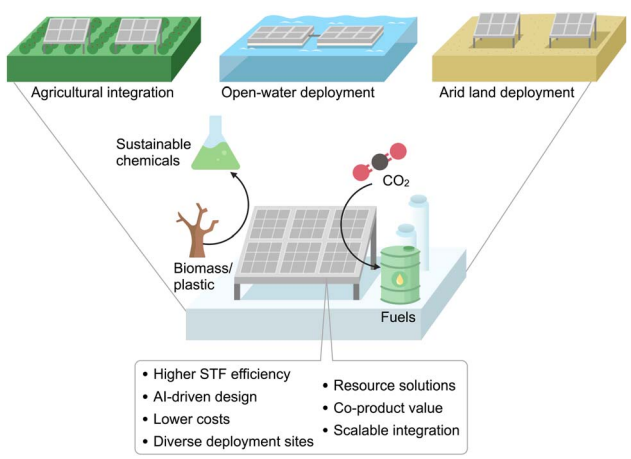

Fig. 6 Future directions for solar-driven CO_2 reduction technologies.

4.3 Enhancing system viability through co-product valorisation

It is suggested that in solar-driven fuel production systems, oxygen evolution must serve as the oxidation product to the reduction of water or CO_2.[14] While this process establishes a closed carbon cycle, the economic contribution of the O_2 by-product is minimal. At a current market price of ~0.1 USD per kg, oxygen sales do little to offset the high capital and operational costs associated with solar-driven CO_2RR systems. For instance, under an STF of 10%, considering the evolved O_2

increases the allowable device cost for CH_4 production from 20 USD per m^2 to ~70 USD per m^2, a value that remains below the threshold needed for commercial viability with currently available CO_2RR systems.

To overcome this limitation, recent efforts have explored replacing the energetically demanding water oxidation half-reaction with thermodynamically more favourable oxidation processes, particularly those involving plastic and biomass waste (Fig. 6).[125,126] These substrates, which include polyethylene terephthalate (PET) and lignocellulosic biomass, can be oxidised under solar irradiation to yield valuable chemicals such as formic acid, glycolic acid or acetic acid. For instance, the photoreforming of ethylene glycol, a monomer derived from PET, offers a compelling case: when its oxidation to formic acid is coupled with CO_2RR to methane, this dual-function system can significantly enhance overall product value and atom economy.[127] The co-generation of formic acid and methane under such conditions shows to increase the allowable device cost to ~490 USD per m^2, a sevenfold increase compared to systems relying on water oxidation (20 USD per m^2, Table 3), assuming the methane production rate remains equivalent to that of a CO_2RR system operating at 10% STF using water as the electron. Importantly, the STF of this co-reforming system will differ from 10%, as the overall reaction ΔG° changes due to the substitution of water with ethylene glycol.

This integrated approach offers several advantages beyond improved economics. It simultaneously addresses global challenges related to plastic pollution, renewable fuel generation and CO_2 utilisation. However, the realisation of such systems at scale demands significant progress in (photo)catalyst development. Specifically, it is essential to design systems that exhibit high selectivity and activity toward the desired products in both the oxidation and reduction half-reactions. Achieving this goal is challenging, as each reaction pathway involves complex multi-electron transfers and is highly sensitive to surface properties and reaction conditions. Additionally, ensuring the compatibility of both catalytic processes under a shared operational window, for example, pH, is crucial for efficient system integration.

5. Conclusions

While the vision of converting CO_2 into solar fuels and chemicals is undeniably compelling and, if realised, would mark a major milestone for sustainable human development, our analysis suggests that solar-driven CO_2RR remains far from achieving commercial-scale deployment. The key bottlenecks include low STF efficiencies and stability, high capital costs of current technologies and insufficient systems integration for scalable implementation.

In the near term, the production of value-added chemicals such as formic acid and acetic acid may offer the most viable entry points for solar-driven CO_2RR deployment. Their relatively high market prices and limited global production volumes create favourable conditions for market penetration and potential disruption. However, significant challenges remain, particularly the energy- and cost-intensive separation of liquid-phase products from aqueous reaction media, which may offset these economic advantages.

By contrast, methane, while representing a scientifically attractive target due to the considerable thermodynamic and kinetic barriers it poses, is far less compelling from a techno-economic standpoint. Its low commercial price and vast global production capacity make it highly unlikely that solar-derived CH_4 by CO_2RR could compete economically in the near future.

Looking ahead, achieving STF efficiencies of 10% or higher will be essential to transform CO_2RR from a laboratory-scale demonstration into a commercially viable solution for renewable fuel production. Achieving this target will require not only innovations in materials but also a paradigm shift that incorporates machine learning and AI-assisted screening and optimisation with advanced *operando* characterisation techniques to elucidate reaction mechanisms and guide design principles. Importantly, this progress hinges on close interdisciplinary collaboration across materials science, surface chemistry, computational modelling, process engineering and systems integration to ensure that data-driven innovations are both scientifically robust and technologically practical.

To bridge the gap between feasibility and deployment, future CO_2RR strategies must integrate catalyst and system design with rigorous techno-economic evaluation. Promising approaches may include deployment in non-traditional environments, such as desert regions or offshore areas, where land use pressures are lower and solar or hybrid renewable resources are abundant. Another compelling strategy involves replacing water oxidation with thermodynamically favourable reactions, such as waste biomass or plastic photoreforming. These processes not only valorise waste streams but also generate high-value oxidation products, substantially improving the cost structure compared to conventional oxygen evolution.

Whether artificial photosynthetic processes can truly power a sustainable future remains an open but increasingly hopeful question. These systems have demonstrated scientific promise across multiple configurations, yet they remain limited by low efficiencies, costly materials and system-level complexity. Nevertheless, with continued innovation in catalyst design, integrated reactor engineering and the use of digital tools for accelerated discovery, artificial photosynthesis may become a practical solution for producing clean fuels and chemicals, particularly in remote, resource-abundant settings where conventional energy systems are less viable. While it may be unlikely to fully displace fossil-based energy, artificial photosynthesis could play a vital complementary role in decarbonising hard-to-electrify sectors and expanding the global portfolio of sustainable energy technologies. We claim that realising the full potential of solar-powered CO_2RR demands a multi-pronged, interdisciplinary approach that goes beyond material development. It requires comprehensive consideration of system performance, economic feasibility, deployment environments and product market integration. Only through close cooperation across scientific and engineering disciplines, guided by data-driven design principles and grounded in techno-economic realities, can CO_2RR evolve into a transformative pillar of the global clean energy economy.

Conflicts of interest

There is no conflicts to declare.

Data availability

The data supporting the findings of this study are available from the corresponding author upon reasonable request.

Acknowledgements

This work was financially supported by the JST Fusion Oriented Research for disruptive Science and Technology Program (GAN JPMJFR213D to Q. W.), JSPS KAKENHI Grant-in-Aid for Scientific Research (B) (GAN JP25K01581 to Q. W.), Foundation of Public Interest of Tatematsu (to Q. W.), the Second Century Fund, Chulalongkorn University (to C. P.), the Grant for development of new faculty stuff, Ratchadaphiseksomphot Fund, Chulalongkorn University (to C. P.), the NSRF *via* the Program Management Unit for Human Resources & Institutional Development, Research and Innovation (GAN B49G680109 to C. P.), The Asahi Glass Foundation (to C. P.), and the Royal Academy of Engineering (GAN FC-2425-5-128 to C. P). This work was supported by the RDP Program Aiming at Maximising the Career Potential of Female Researchers, Nagoya University, (MEXT's Initiative for Realising Diversity in the Research Environment, Leadership training type for women). We acknowledge the use of English editing tools, including Grammarly and ChatGPT, for refining the language and assisting with grammar correction in this manuscript.

References

1 M. Reichstein, M. Bahn, P. Ciais, D. Frank, M. D. Mahecha, S. I. Seneviratne, J. Zscheischler, C. Beer, N. Buchmann, D. C. Frank, D. Papale, A. Rammig, P. Smith, K. Thonicke, M. van der Velde, S. Vicca, A. Walz and M. Wattenbach, *Nature*, 2013, **500**, 287–295.
2 J. Gao, J. Li, Y. Liu, M. Xia, Y. Z. Finfrock, S. M. Zakeeruddin, D. Ren and M. Grätzel, *Nat. Commun.*, 2022, **13**, 5898.
3 B. A. Pinaud, J. D. Benck, L. C. Seitz, A. J. Forman, Z. Chen, T. G. Deutsch, B. D. James, K. N. Baum, G. N. Baum and S. Ardo, *Energy Environ. Sci.*, 2013, **6**, 1983–2002.
4 D. M. Fabian, S. Hu, N. Singh, F. A. Houle, T. Hisatomi, K. Domen, F. E. Osterloh and S. Ardo, *Energy Environ. Sci.*, 2015, **8**, 2825–2850.
5 M. R. Shaner, H. A. Atwater, N. S. Lewis and E. W. McFarland, *Energy Environ. Sci.*, 2016, **9**, 2354–2371.
6 H. Nakanishi, K. Iizuka, T. Takayama, A. Iwase and A. Kudo, *ChemSusChem*, 2017, **10**, 112–118.
7 S. Wang, K. Teramura, T. Hisatomi, K. Domen, H. Asakura, S. Hosokawa and T. Tanaka, *ACS Sustain. Chem. Eng.*, 2021, **9**, 9327–9335.
8 M. G. Walter, E. L. Warren, J. R. McKone, S. W. Boettcher, Q. Mi, E. A. Santori and N. S. Lewis, *Chem. Rev.*, 2010, **110**, 6446–6473.
9 J. Ran, M. Jaroniec and S.-Z. Qiao, *Adv. Mater.*, 2018, **30**, 1704649.
10 Y. Wang, H. Suzuki, J. Xie, O. Tomita, D. J. Martin, M. Higashi, D. Kong, R. Abe and J. Tang, *Chem. Rev.*, 2018, **118**, 5201–5241.
11 Q. Wang, J. Warnan, S. Rodríguez-Jiménez, J. J. Leung, S. Kalathil, V. Andrei, K. Domen and E. Reisner, *Nat. Energy*, 2020, **5**, 703–710.
12 S. Hu, C. Xiang, S. Haussener, A. D. Berger and N. S. Lewis, *Energy Environ. Sci.*, 2013, **6**, 2984–2993.
13 T. Arai, S. Sato, T. Kajino and T. Morikawa, *Energy Environ. Sci.*, 2013, **6**, 1274–1282.
14 N. S. Lewis and D. G. Nocera, *Proc. Natl. Acad. Sci. U. S. A.*, 2006, **103**, 15729–15735.
15 X. Chang, T. Wang and J. Gong, *Energy Environ. Sci.*, 2016, **9**, 2177–2196.
16 Q. Wang and Z. Pan, *Nano Res.*, 2022, **15**, 10090–10109.
17 J. B. Greenblatt, D. J. Miller, J. W. Ager, F. A. Houle and I. D. Sharp, *Joule*, 2018, **2**, 381–420.
18 S. J. Cobb, C. Pornrungroj, V. Andrei, V. M. Badiani, L. Su, R. R. Manuel, I. A. C. Pereira and E. Reisner, *Device*, 2024, **2**, 100505.
19 K. Iizuka, T. Wato, Y. Miseki, K. Saito and A. Kudo, *J. Am. Chem. Soc.*, 2011, **133**, 20863–20868.
20 S. Wang, K. Teramura, T. Hisatomi, K. Domen, H. Asakura, S. Hosokawa and T. Tanaka, *ChemistrySelect*, 2020, **5**, 8779–8786.
21 Y. Y. Birdja, E. Pérez-Gallent, M. C. Figueiredo, A. J. Göttle, F. Calle-Vallejo and M. T. M. Koper, *Nat. Energy*, 2019, **4**, 732–745.
22 K. Li, B. Peng and T. Peng, *ACS Catal.*, 2016, **6**, 7485–7527.
23 Z. Wang, K. Teramura, S. Hosokawa and T. Tanaka, *J. Mater. Chem. A*, 2015, **3**, 11313–11319.
24 J. Albero, Y. Peng and H. García, *ACS Catal.*, 2020, **10**, 5734–5749.
25 S. Nitopi, E. Bertheussen, S. B. Scott, X. Liu, A. K. Engstfeld, S. Horch, B. Seger, I. E. L. Stephens, K. Chan, C. Hahn, J. K. Nørskov, T. F. Jaramillo and I. Chorkendorff, *Chem. Rev.*, 2019, **119**, 7610–7672.
26 H. Mistry, F. Behafarid, R. Reske, A. S. Varela, P. Strasser and B. Roldan Cuenya, *ACS Catal.*, 2016, **6**, 1075–1080.
27 D. Gao, R. M. Arán-Ais, H. S. Jeon and B. Roldan Cuenya, *Nat. Catal.*, 2019, **2**, 198–210.
28 X. K. Lu and L. C. Seitz, *Chem. Soc. Rev.*, 2025, **54**, 6088–6121.
29 F. Pan, X. Yang, T. O'Carroll, H. Li, K.-J. Chen and G. Wu, *Adv. Energy Mater.*, 2022, **12**, 2200586.
30 J. Wang, S. Lin, N. Tian, T. Ma, Y. Zhang and H. Huang, *Adv. Funct. Mater.*, 2021, **31**, 2008008.
31 M. Li, H. Wang, W. Luo, P. C. Sherrell, J. Chen and J. Yang, *Adv. Mater.*, 2020, **32**, 2001848.
32 Y. Zhao, J. Zhang, X. Guo, X. Cao, S. Wang, H. Liu and G. Wang, *Chem. Soc. Rev.*, 2023, **52**, 3215–3264.
33 S. Zhu, E. P. Delmo, T. Li, X. Qin, J. Tian, L. Zhang and M. Shao, *Adv. Mater.*, 2021, **33**, 2005484.
34 B. Chang, H. Pang, F. Raziq, S. Wang, K.-W. Huang, J. Ye and H. Zhang, *Energy Environ. Sci.*, 2023, **16**, 4714–4758.

35 A. Wagner, C. D. Sahm and E. Reisner, *Nat. Catal.*, 2020, **3**, 775–786.
36 K. E. Dalle, J. Warnan, J. J. Leung, B. Reuillard, I. S. Karmel and E. Reisner, *Chem. Rev.*, 2019, **119**, 2752–2875.
37 M. Cokoja, C. Bruckmeier, B. Rieger, W. A. Herrmann and F. E. Kühn, *Angew. Chem., Int. Ed.*, 2011, **50**, 8510–8537.
38 A. J. Morris, G. J. Meyer and E. Fujita, *Acc. Chem. Res.*, 2009, **42**, 1983–1994.
39 W. Leitner, *Coord. Chem. Rev.*, 1996, **153**, 257–284.
40 C. D. Windle and E. Reisner, *Chimia*, 2015, **69**, 435–441.
41 H. Kumagai, G. Sahara, K. Maeda, M. Higashi, R. Abe and O. Ishitani, *Chem. Sci.*, 2017, **8**, 4242–4249.
42 S. Schlager, A. Dibenedetto, M. Aresta, D. H. Apaydin, L. M. Dumitru, H. Neugebauer and N. S. Sariciftci, *Energy Technol.*, 2017, **5**, 812–821.
43 P. Singh and R. Srivastava, *J. CO2 Util.*, 2021, **53**, 101748.
44 F. B. H. Rehm, S. Chen and B. H. A. Rehm, *Bioengineered*, 2018, **9**, 6–11.
45 L. Lapinsonnière, M. Picot and F. Barrière, *ChemSusChem*, 2012, **5**, 995–1005.
46 H. Li, P. H. Opgenorth, D. G. Wernick, S. Rogers, T.-Y. Wu, W. Higashide, P. Malati, Y.-X. Huo, K. M. Cho and J. C. Liao, *Science*, 2012, **335**, 1596.
47 K. K. Sakimoto, A. B. Wong and P. Yang, *Science*, 2016, **351**, 74–77.
48 N. Kornienko, J. Z. Zhang, K. K. Sakimoto, P. Yang and E. Reisner, *Nat. Nanotechnol.*, 2018, **13**, 890–899.
49 International Energy Agency (IEA), *CO2 Emissions in 2023*, **https://www.iea.org/reports/co2-emissions-in-2023**, accessed May 2025.
50 S. Kar, M. Rahaman, V. Andrei, S. Bhattacharjee, S. Roy and E. Reisner, *Joule*, 2023, **7**, 1496–1514.
51 E. S. Rubin, J. E. Davison and H. J. Herzog, *Int. J. Greenhouse Gas Control*, 2015, **40**, 378–400.
52 A. Álvarez, A. Bansode, A. Urakawa, A. V. Bavykina, T. A. Wezendonk, M. Makkee, J. Gascon and F. Kapteijn, *Chem. Rev.*, 2017, **117**, 9804–9838.
53 M. Fasihi, O. Efimova and C. Breyer, *J. Cleaner Prod.*, 2019, **224**, 957–980.
54 S. Kar, D. Kim, A. Bin Mohamad Annuar, B. B. Sarma, M. Stanton, E. Lam, S. Bhattacharjee, S. Karak, H. F. Greer and E. Reisner, *Nat. Energy*, 2025, **10**, 448–459.
55 H. Nishiyama, T. Yamada, M. Nakabayashi, Y. Maehara, M. Yamaguchi, Y. Kuromiya, H. Tokudome, S. Akiyama, T. Watanabe, R. Narushima, S. Okunaka, N. Shibata, T. Takata, T. Hisatomi and K. Domen, *Nature*, 2021, **598**, 304–307.
56 H. Phong Duong, J. G. Rivera de la Cruz, D. Portehault, A. Zitolo, J. Louis, S. Zanna, Q. Arnoux, M. W. Schreiber, N. Menguy, N.-H. Tran and M. Fontecave, *Nat. Mater.*, 2025, **24**, 900–906.
57 T. Haas, R. Krause, R. Weber, M. Demler and G. Schmid, *Nat. Catal.*, 2018, **1**, 32–39.
58 L. Li, A. Ozden, S. Guo, F. P. García de Arquer, C. Wang, M. Zhang, J. Zhang, H. Jiang, W. Wang, H. Dong, D. Sinton, E. H. Sargent and M. Zhong, *Nat. Commun.*, 2021, **12**, 5223.
59 N. Kato, S. Mizuno, M. Shiozawa, N. Nojiri, Y. Kawai, K. Fukumoto, T. Morikawa and Y. Takeda, *Joule*, 2021, **5**, 687–705.
60 V. Andrei, Y.-H. Chiang, M. Rahaman, M. Anaya, T. Kang, E. Ruggeri, S. D. Stranks and E. Reisner, *Energy Environ. Sci.*, 2025, **18**, 3623–3632.
61 Q. Wang, T. Hisatomi, Y. Suzuki, Z. Pan, J. Seo, M. Katayama, T. Minegishi, H. Nishiyama, T. Takata, K. Seki, A. Kudo, T. Yamada and K. Domen, *J. Am. Chem. Soc.*, 2017, **139**, 1675–1683.
62 X. Yao, D. Wang, X. Zhao, S. Ma, P. S. Bassi, G. Yang, W. Chen, Z. Chen and T. Sritharan, *Energy Technol.*, 2018, **6**, 100–109.
63 C. Pornrungroj, V. Andrei and E. Reisner, *J. Am. Chem. Soc.*, 2023, **145**, 13709–13714.
64 I. Y. Ahmet, Y. Ma, J.-W. Jang, T. Henschel, B. Stannowski, T. Lopes, A. Vilanova, A. Mendes, F. F. Abdi and R. van de Krol, *Sustainable Energy Fuels*, 2019, **3**, 2366–2379.
65 T. Higashi, H. Kaneko, T. Minegishi, H. Kobayashi, M. Zhong, Y. Kuang, T. Hisatomi, M. Katayama, T. Takata, H. Nishiyama, T. Yamada and K. Domen, *Chem. Commun.*, 2017, **53**, 11674–11677.
66 V. E. Nelson, C. P. O'Brien, J. P. Edwards, S. Liu, C. M. Gabardo, E. H. Sargent and D. Sinton, *ACS Appl. Mater. Interfaces*, 2024, **16**, 50818–50825.
67 Z. Wang, T. Hisatomi, R. Li, K. Sayama, G. Liu, K. Domen, C. Li and L. Wang, *Joule*, 2021, **5**, 344–359.
68 A. Kudo and Y. Miseki, *Chem. Soc. Rev.*, 2009, **38**, 253–278.
69 M. Qureshi and K. Takanabe, *Chem. Mater.*, 2016, **29**, 158–167.
70 F. E. Osterloh, *ACS Energy Lett.*, 2017, **2**, 445–453.
71 K. Teramura, K. Hori, Y. Terao, Z. Huang, S. Iguchi, Z. Wang, H. Asakura, S. Hosokawa and T. Tanaka, *J. Phys. Chem. C*, 2017, **121**, 8711–8721.
72 Global Market Insights, **https://www.gminsights.com/industry-analysis/formic-acid-market**, accessed May 2025.
73 Market Research Future, **https://www.marketresearchfuture.com/reports/formic-acid-market-1132**, accessed May 2025.
74 Fortune Business Insights, **https://www.fortunebusinessinsights.com/carbon-monoxide-market-105343**, accessed May 2025.
75 Grand View Research, **https://www.grandviewresearch.com/industry-analysis/syngas-market-report**, accessed May 2025.
76 P. Wang, F.-K. Chiang, J. Chai, A. I. Dugulan, J. Dong, W. Chen, R. J. P. Broos, B. Feng, Y. Song, Y. Lv, Q. Lin, R. Wang, I. A. W. Filot, Z. Men and E. J. M. Hensen, *Nature*, 2024, **635**, 102–107.
77 Market Research Future, **https://www.marketresearchfuture.com/reports/ethane-market-7372**, accessed May 2025.
78 Grand View Research, **https://www.grandviewresearch.com/industry-analysis/acetic-acid-market**, accessed May 2025.

79 Fortune Business Insights, https://www.fortunebusinessinsights.com/industry-reports/methanol-market-101552, accessed May 2025.
80 Fortune Business Insights, https://www.fortunebusinessinsights.com/industry-reports/ethanol-market-101567, accessed May 2025.
81 J.-G. Rosenboom, R. Langer and G. Traverso, *Nat. Rev. Mater.*, 2022, **7**, 117–137.
82 Market Research Future, https://www.marketresearchfuture.com/reports/methane-market-7373, accessed May 2025.
83 Fortune Business Insights, https://www.fortunebusinessinsights.com/ethylene-market-104532, accessed May 2025.
84 Market Research Future, https://www.marketresearchfuture.com/reports/ethylene-market-931, accessed May 2025.
85 Grand View Research, https://www.grandviewresearch.com/industry-analysis/hydrogen-generation-market, accessed May 2025.
86 Market and Market, https://www.marketsandmarkets.com/Market-Reports/hydrogen-market-132975342.html, accessed May 2025.
87 International Energy Agency (IEA), *Global Hydrogen Review 2024*, https://iea.blob.core.windows.net/assets/89c1e382-dc59-46ca-aa47-9f7d41531ab5/GlobalHydrogenReview2024.pdf, accessed May 2025.
88 T. Hisatomi and K. Domen, *Nat. Catal.*, 2019, **2**, 387–399.
89 The National Renewable Energy Laboratory Economic Feasibility for CO2 Utilization Data Visualization Tool, https://www.nrel.gov/bioenergy/co2-utilization-economics/electrochemical-conversion-pathway, accessed May 2025.
90 Market Research Future, https://www.marketresearchfuture.com/reports/syngas-market-7487, accessed May 2025.
91 M. Moreno-Gonzalez, A. Berger, T. Borsboom-Hanson and W. Mérida, *Energy Convers. Manage.*, 2021, **244**, 114452.
92 Fortune Business Insights, https://www.fortunebusinessinsights.com/syngas-market-109820, accessed May 2025.
93 R. Detz, M. Beerse, N. Meulendijks, P. Buskens and B. van der Zwaan, *ChemSusChem*, 2024, **17**, e202400059.
94 The International Energy Agency (IEA), *U.S. Ethane Production, Consumption, and Exports Set New Records in 2024*, https://www.eia.gov/todayinenergy/detail.php?id=64785, accessed May 2025.
95 Statista, https://www.statista.com/statistics/1170573/price-ethylene-forecast-globally/, accessed May 2025.
96 Business Analytiq, https://businessanalytiq.com/procurementanalytics/index/acetic-acid-price-index/, accessed May 2025.
97 Statista, https://www.statista.com/statistics/1245203/acetic-acid-market-volume-worldwide/, accessed May 2025.
98 T. Nakyai and D. Saebea, *J. Cleaner Prod.*, 2019, **241**, 118334.
99 Q. Wang and K. Domen, *Chem. Rev.*, 2019, **120**, 919–985.
100 A. Cattry, H. Johnson, D. Chatzikiriakou and S. Haussener, *Energy Fuels*, 2024, **38**, 12058–12077.
101 Y. Cao, Z. Gao, J. Jin, H. Zhou, M. Cohron, H. Zhao, H. Liu and W. Pan, *Energy Fuels*, 2008, **22**, 1720–1730.
102 Q. Wang, T. Hisatomi, Q. Jia, H. Tokudome, M. Zhong, C. Wang, Z. Pan, T. Takata, M. Nakabayashi, N. Shibata, Y. Li, I. D. Sharp, A. Kudo, T. Yamada and K. Domen, *Nat. Mater.*, 2016, **15**, 611–615.
103 T. A. Kistler, M. Y. Um, J. K. Cooper, I. D. Sharp and P. Agbo, *Adv. Energy Mater.*, 2021, **11**, 2100070.
104 B. Khan, M. B. Faheem, K. Peramaiah, J. Nie, H. Huang, Z. Li, C. Liu, K.-W. Huang and J.-H. He, *Nat. Commun.*, 2024, **15**, 6990.
105 K. Su, W. Wang, S. Du, C. Ji and D. Yuan, *Nat. Commun.*, 2021, **12**, 3703.
106 B. Wu, L. D. Voleti, A. Q. Fenwick, C. Wu, J. Zhang, N. Ling, M. Wang, Y. Jia, W. W. Tjiu, M. Zhang, Z. Aabdin, S. Xi, C. S. Mathpati, S. Zhang, H. A. Atwater, I. A. Karimi and Y. Lum, *EES Catal.*, 2025, **3**, 318–326.
107 M. Ramdin, A. R. T. Morrison, M. de Groen, R. van Haperen, R. de Kler, E. Irtem, A. T. Laitinen, L. J. P. van den Broeke, T. Breugelmans, J. P. M. Trusler, W. d. Jong and T. J. H. Vlugt, *Ind. Eng. Chem. Res.*, 2019, **58**, 22718–22740.
108 D. Van Baelen, B. Van der Bruggen, K. Van den Dungen, J. Degreve and C. Vandecasteele, *Chem. Eng. Sci.*, 2005, **60**, 1583–1590.
109 P. Wang, A. Pei, Z. Chen, P. Sun, C. Hu, X. Wang, N. Zheng and G. Chen, *Nat. Commun.*, 2025, **16**, 731.
110 R. Chen, Z. Ren, Y. Liang, G. Zhang, T. Dittrich, R. Liu, Y. Liu, Y. Zhao, S. Pang, H. An, C. Ni, P. Zhou, K. Han, F. Fan and C. Li, *Nature*, 2022, **610**, 296–301.
111 Y. Wang, A. Vogel, M. Sachs, R. S. Sprick, L. Wilbraham, S. J. A. Moniz, R. Godin, M. A. Zwijnenburg, J. R. Durrant, A. I. Cooper and J. Tang, *Nat. Energy*, 2019, **4**, 746–760.
112 H. Zhang, C. Xu, X. Zhan, Y. Yu, K. Zhang, Q. Luo, S. Gao, J. Yang and Y. Xie, *Nat. Commun.*, 2022, **13**, 6029.
113 C. Lin, J.-L. Li, X. Li, S. Yang, W. Luo, Y. Zhang, S.-H. Kim, D.-H. Kim, S. S. Shinde, Y.-F. Li, Z.-P. Liu, Z. Jiang and J.-H. Lee, *Nat. Catal.*, 2021, **4**, 1012–1023.
114 B. Samanta, Á. Morales-García, F. Illas, N. Goga, J. A. Anta, S. Calero, A. Bieberle-Hütter, F. Libisch, A. B. Muñoz-García, M. Pavone and M. Caspary Toroker, *Chem. Soc. Rev.*, 2022, **51**, 3794–3818.
115 B. Burger, P. M. Maffettone, V. V. Gusev, C. M. Aitchison, Y. Bai, X. Wang, X. Li, B. M. Alston, B. Li, R. Clowes, N. Rankin, B. Harris, R. S. Sprick and A. I. Cooper, *Nature*, 2020, **583**, 237–241.
116 Y. Chu, Y. Wang, D. Zhang, X. Song, C. Yu and H. Li, *J. Chem. Phys.*, 2025, **162**, 174703.
117 M. Rittiruam, P. Khamloet, A. Ektarawong, C. Atthapak, T. Saelee, P. Khajondetchairit, B. Alling, S. Praserthdam and P. Praserthdam, *Appl. Surf. Sci.*, 2024, **652**, 159297.
118 S. Ma Lu, S. Amaducci, S. Gorjian, M. Haworth, C. Hägglund, T. Ma, S. Zainali and P. E. Campana, *Joule*, 2024, **8**, 2483–2522.
119 X. Xu, K. Vignarooban, B. Xu, K. Hsu and A. M. Kannan, *Renewable Sustainable Energy Rev.*, 2016, **53**, 1106–1131.

120 L. Zhai, M. C. Berg, F. Ç. Cebeci, Y. Kim, J. M. Milwid, M. F. Rubner and R. E. Cohen, *Nano Lett.*, 2006, **6**, 1213–1217.
121 W. Song, Z. Zheng, A. H. Alawadhi and O. M. Yaghi, *Nat. Water*, 2023, **1**, 626–634.
122 M. W. Logan, S. Langevin and Z. Xia, *Sci. Rep.*, 2020, **10**, 1492.
123 V. Andrei, G. M. Ucoski, C. Pornrungroj, C. Uswachoke, Q. Wang, D. S. Achilleos, H. Kasap, K. P. Sokol, R. A. Jagt, H. Lu, T. Lawson, A. Wagner, S. D. Pike, D. S. Wright, R. L. Z. Hoye, J. L. MacManus-Driscoll, H. J. Joyce, R. H. Friend and E. Reisner, *Nature*, 2022, **608**, 518–522.
124 Y. Jin, S. Hu, A. D. Ziegler, L. Gibson, J. E. Campbell, R. Xu, D. Chen, K. Zhu, Y. Zheng, B. Ye, F. Ye and Z. Zeng, *Nat. Sustain.*, 2023, **6**, 865–874.
125 Z. Huang, N. Luo, C. Zhang and F. Wang, *Nat. Rev. Chem.*, 2022, **6**, 197–214.
126 T. K. Anh Nguyen, T. Trân-Phú, R. Daiyan, X. Minh Chau Ta, R. Amal and A. Tricoli, *Angew. Chem., Int. Ed.*, 2024, **63**, e202401746.
127 Y. Liu, C. W. S. Yeung and E. Reisner, *Energy Environ. Sci.*, 2025, **18**, 7023–7033.